Regulatory T Cells Control Th2-Dominant Murine Autoimmune Gastritis[1]

Jessica Harakal[*,‡], **Claudia Rival**[*,†,‡], **Hui Qiao**[†,‡], and **Kenneth S. Tung**[*,†,‡]

[*]Department of Microbiology, Immunology, and Cancer Biology, University of Virginia, Charlottesville, VA 22908

[†]Department of Pathology, University of Virginia, Charlottesville, VA 22908

[‡]Beirne B. Carter Center for Immunology Research, University of Virginia, Charlottesville, VA 22908

Abstract

Pernicious anemia and gastric carcinoma are serious sequelae of autoimmune gastritis (AIG). Our study indicates that in adult C57BL/6 DEREG mice expressing a transgenic diphtheria toxin receptor under the *Foxp3* promoter, transient Treg cell depletion results in long-lasting AIG associated with both $H^+K^+ATPase$ and intrinsic factor autoantibody responses. Although functional Treg cells emerge over time during AIG occurrence, the effector T cells rapidly become less susceptible to Treg cell-mediated suppression. While previous studies have implicated dysregulated Th1 responses in AIG pathogenesis, eosinophils have been detected in gastric biopsies from patients with AIG. Indeed, AIG in DEREG mice is associated with strong Th2 responses, including dominant IgG1 autoantibodies, elevated serum IgE, increased Th2 cytokine production, and eosinophil infiltration in the stomach draining lymph nodes. Additionally, the stomachs exhibit severe mucosal and muscular hypertrophy, parietal cell loss, mucinous epithelial cell metaplasia, and massive eosinophilic inflammation. Notably, the Th2 responses and gastritis severity are significantly ameliorated in IL-4- or eosinophil-deficient mice. Furthermore, expansion of both Th2-promoting IRF4+PD-L2+ dendritic cells and ILT3+ rebounded Treg cells were detected after transient Treg cell depletion. Collectively, these data suggest that Treg cells maintain physiological tolerance to clinically relevant gastric autoantigens, and Th2 responses can be a pathogenic mechanism in autoimmune gastritis.

Keywords

Autoantibodies; Autoimmunity; Eosinophils; Rodent; Stomach; Th2 cells; Tolerance/Suppression

Introduction

An essential function of the immune system is to distinguish foreign from self-antigens, allowing for protection from invading pathogens while preventing autoimmune responses. T cell tolerance, initiated in the thymus, is maintained by the peripheral lymphoid organs in communication with local tissue and environmental factors, such as those existing in the skin and mucosal sites (1). The cellular mechanisms include T cell deletion, anergy, and suppression by regulatory T (Treg) cells, which likely operate in concert to fully maintain the tolerance state. CD4+Foxp3+ Treg cells play a critical role in maintaining immune homeostasis and tolerance to self-antigens by suppressing effector T cell and innate cell activities (2). The transcription factor Foxp3 is required for Treg cell development and function (3–5). Loss-of-function mutations in *Foxp3* lead to scurfy syndrome in mice that exhibit progressive fatal multiorgan auto-inflammation (6, 7) and the immune dysregulation, polyendocrinopathy, enteropathy, X-linked (IPEX) syndrome in patients (8, 9).

Autoimmune gastritis (AIG) is a common disease of the stomach associated with autoantibodies that target intrinsic factor (IF), which supports vitamin B12 absorption, and the gastric $H^+K^+ATPase$, the proton pump expressed by acid-secreting parietal cells in gastric glands (10–15). Accordingly, AIG patients are predisposed to the development of gastric cancer (16–18) and pernicious anemia, the most common sequela of vitamin B12 deficiency, which has an estimated prevalence of ~1.9% among the elderly Western population (19, 20). The histological characterization of active human AIG includes immune cell infiltration in the corpus and body regions of the stomach and loss of gastric zymogenic and parietal cells (21). Because of their strong resemblance to the human disease, murine AIG models have been frequently utilized for research on tolerance and mechanisms of organ-specific autoimmune disease.

Experimental AIG research has focused on addressing whether a defect in tolerance mechanisms, such as Treg cells, is the underpinning of human autoimmune diseases and the rationale behind Treg cell-based therapies. For many years, this question has been investigated in the day 3 thymectomy (d3tx) model of BALB/c mice (22–25). It was thought that Treg cells exit the thymus after the non-Treg T cells and should be preferentially depleted by thymectomy between neonatal days 1–5 (26–29). This idea was supported by the blockade of AIG by transfer of normal Treg cells soon after thymectomy (22, 24, 30, 31). However, more recent studies have yielded new findings inconsistent with this concept: 1) Treg cells with the capacity to suppress autoimmune disease were detected in the lymph nodes and spleen before day 3 (32), 2) d3tx led to an increase, rather than a reduction, of functional Treg cell fractions (33, 34), 3) Treg cell depletion by anti-CD25 antibody (PC61) in d3tx mice greatly enhanced the AIG immunopathology (34, 35), and 4) d3tx mice developed severe lymphopenia, and the attendant homeostatic expansion of the autoreactive effector T cell compartment, including gastritogenic T cell clones, could also contribute to disease (26, 34, 36–38).

To more directly address Treg cell depletion without the confounding lymphopenic state, recent studies have turned to genetically modified mouse lines expressing the diphtheria toxin receptor (DTR) under the control of a *Foxp3* promoter, from which Treg cells can be

depleted by diphtheria toxin (DT) treatment. In both neonatal and adult Foxp3[DTR] knock-in mice, continuous DT treatment led to dramatic expansion and activation of adaptive and innate cells, a scurfy-like phenotype, and death of unknown cause by 3–4 weeks (39). Adult BALB/c Foxp3[DTR] mice with transient Treg cell depletion also suffered from death within 4–5 weeks. Moreover, despite the re-emergence of Treg cells, the mice exhibited rapidly increased cytokine production, enhanced antigen-specific T cell activation, development of AIG with mononuclear cell infiltration, and parietal cell autoantibody responses (40). These findings raise the critical questions of whether transient Treg cell deficiency is sufficient to induce AIG, and why the restored Treg cell population fails to maintain tolerance (41).

In addition to the Foxp3[DTR] knock-in mice, recent studies were conducted with the DEREG (DEpletion of REGulatory T cells) mice that express a bacterial artificial chromosome containing a DTR and enhanced GFP fusion protein. While DT-treated newborn C57BL/6 DEREG mice develop scurfy-like syndrome, adult C57BL/6 and BALB/c DEREG mice were reportedly free of pathology after transient Treg cell depletion (42, 43). This lack of pathology was attributed to the maintenance of tolerance by a minor population of residual DT-insensitive Treg cells. Adult BALB/c DEREG mice crossed with the Foxp3[GFP] mice also failed to induce AIG, but blepharitis and scurfy-like auto-inflammation were detected (43). However, unlike the Foxp3[DTR] knock-in mice, the adult DEREG mice with transient Treg cell depletion did not succumb to early fatality (42, 44).

In order to develop an AIG model that is more suitable for detailed mechanistic analyses, we have conducted studies using the C57BL/6 DEREG mice, kindly donated by Drs. Lahl and Sparwassar, to systematically examine autoimmune disease development after transient Treg cell depletion. Contrary to previous findings, the study in our laboratory revealed that adult DT-treated C57BL/6 DEREG mice developed frequent and severe AIG that persisted for at least 16 weeks. We found that after Treg cell depletion, the non-Treg T cells rapidly became less susceptible to Treg cell-mediated suppression. This finding provides a tangible explanation for the failure of the functional rebounded Treg cell population to control AIG. Moreover, AIG that develops in the adult DEREG model exhibited a unique antibody response and immunopathology indicative of a robust Th2-dominant autoimmune response dependent on IL-4 and eosinophils.

Materials and Methods

Mice and Foxp3+ Treg cell depletion

C57BL/6-DEREG mice were kindly provided by Drs. Lahl and Sparwasser (Twin Core). A/J mice, C57BL/6 Rag1$^{-/-}$ mice, and C57BL/6 IL-4$^{-/-}$ mice were purchased from The Jackson Laboratory. C57BL/6 PHIL mice were generously provided by James Lee (Mayo Clinic). Rag1$^{-/-}$ DEREG mice were generated by crossing Rag1$^{-/-}$ mice with DEREG mice. IL-4$^{-/-}$ DEREG and DEREG PHIL mice were generated by crossing the DEREG mice with the IL-4$^{-/-}$ or the PHIL mice, respectively. To obtain B6AF1-DEREG mice, C57BL/6-DEREG mice were crossed with A/J mice. To deplete Treg cells, 40μg/kg body weight of diphtheria toxin (DT) (Lot 322326, Calbiochem) was injected intraperitoneally into 6–12 week old DEREG mice on days 0, 2, and 5. All experimental days were counted from day 0. As a control, we studied WT mice injected with DT and DEREG mice injected with PBS. All

mice were bred in house in a specific pathogen-free facility and tested negative for fur mites, pinworm infection, and *Helicobacter* spp. infections. Experiments were conducted following the guidelines of the Animal Care and Use Committee of the University of Virginia.

Histopathology and AIG severity grading

Mice were euthanized from 1 to 16 weeks after Treg cell depletion. The stomachs were weighed after the removal of gastric contents, then fixed in Bouin's solution, embedded in paraffin wax, and cut into 5um-thick sections. The presence of inflammation and parietal cells were examined by H&E stain, and mucin-positive cells were identified by Periodic acid-Schiff/hematoxylin stain. AIG was graded as unknown samples. AIG severity score was determined by the summation of the extent of inflammation, parietal cell loss, and mucinous cell hyperplasia. Each change was assigned a grade of 0 (none), 1 (mild), 2 (moderate), 3 (moderate and diffuse or severe but focal), or 4 (severe and diffuse). Because parietal cell loss and mucinous cell hyperplasia are structural changes and likely associated with loss of gastric function, we multiplied their scores by a factor of 1.5. Therefore, the total AIG scores ranged from 0 to 16.

Immunofluorescence microscopy

Serum gastric autoantibodies were detected and semi-quantified by indirect immunofluorescence staining of 6um-thick frozen sections of normal mouse stomach pre-fixed in 1% periodate-lysine-paraformaldehyde. After the sections were blocked with PBS containing normal goat serum and 3% BSA, they were incubated with serum from control or Treg cell-depleted mice, followed by incubation with FITC-conjugated goat anti-mouse IgG (Jackson Immunoresearch Laboratories), anti-mouse IgG1 (Southern Biotech), or anti-mouse IgG2a (Southern Biotech). Staining intensity was scored as 0 (negative) to 3 (most positive). To study IF autoantibodies, mouse sera were costained with IF antibody, a generous gift from David Alpers (Washington University, St Louis), on normal stomach sections. Mouse sera staining (described above) was detected with AlexaFluor488-conjugated rabbit anti-mouse IgG (Jackson ImmunoResearch Laboratories) followed by blockade with a biotin-avidin blocking kit (Vector Laboratories) and co-stained with goat anti-human IF antibody followed by biotinylated horse anti-goat IgG (Vector Laboratories) and neutralite avidin-Texas Red (Southern Biotech). To detect eosinophils by direct immunofluorescence, 6μm frozen stomach sections were fixed in cold 1:1 acetone:ethanol and blocked with Tris-NaCl blocking buffer (PerkinElmer), 3% H_2O_2 (EMD Chemicals), 0.1% NaN_3 (ICN Biomedicals, Inc), followed by a biotin-avidin blocking kit. The sections were then stained with rat anti-mouse SiglecF antibody (BD-Pharmingen) and biotinylated goat anti-rat IgG (Southern Biotech). Then, staining was enhanced by the biotin tyramide kit according to the manufacturer's instructions (PerkinElmer), followed by neutralite avidin-Texas Red. To detect parietal cells on the same sections, the slides were then co-stained with DEREG mouse serum antibody to parietal cell antigens as described above and mounted with Vectashield containing DAPI (Vector Laboratories). Unless noted otherwise, all stains were performed at room temperature and the slides were examined and photographed with a Nikon Microphot-FXA fluorescent microscope and Nikon HB-10101AF Mercury Lamp and Olympus Q color 5 camera. Alternatively, they were examined with a Zeiss LSM 700 confocal microscope or a Zeiss Axio Observer microscope with Qioptiq OptiGrid.

ELISA detection of gastric H⁺K⁺ATPase antibody and IF antibody

To detect H^+K^+ATPase antibody, 96-well plates were incubated with 0.5μg/mL H^+K^+ATPase (Arotec Diagnostics) in 10mM Tris-HCL (pH 8)/0.15 M NaCl/0.1% sodium desoxycholate for 16h at 4°C. The wells were blocked with PBS containing 1% BSA for 1h at 37°C. Experimental and control mouse sera were added to the wells at 1:50 and 1:100 dilutions in duplicate and incubated for 1h at room temperature. The wells were then incubated with horseradish peroxidase-conjugated goat anti-mouse IgG (Southern Biotech) diluted 1:2000 for 1h at room temperature. After rigorous washing, each well was reacted with OPD substrate solution (Sigma-Aldrich). The reaction was terminated with 2.5N H_2SO_4, and absorbance at 490nm was determined with a microplate reader. H^+K^+ATPase concentrations were expressed as arbitrary units relative to a standard curve.

To detect IF antibody, 96-well plates were coated with 5μg/mL recombinant rat IF (Cloud-Clone Corp.) in 0.5M Na_2HCO_3 for 4h at room temperature and blocked with PBS containing 0.05% Tween20 overnight. Experimental and control mouse sera were added to the wells at 1:50 dilutions for 1h. The wells were then incubated with horseradish peroxidase-conjugated goat anti-mouse IgG (Southern Biotech) diluted 1:2000 for 1h. As a positive control, a goat anti-human IF antibody (provided by David Alpers, Washington University, St Louis) was added for 1h, followed by biotinylated horse anti-goat IgG (Vector Laboratories) diluted 1:200 for 1h, and streptavidin-conjugated horseradish peroxidase (Perkin Elmer Life Sciences) diluted 1:1000 for 1h. All incubations were performed at room temperature. After rigorous washing, each well was reacted with OPD substrate solution. The reaction was terminated with 2.5N H_2SO_4, and absorbance at 490nm was determined with a microplate reader.

Serum IgE determination by ELISA

96-well plates were coated overnight with 5μg/mL unlabeled goat anti-mouse IgE (Southern Biotech) in PBS. After blocking and 2h incubation with serum samples at 1:200 and 1:400 dilutions in duplicate, the wells were incubated with horseradish peroxidase-conjugated goat anti-mouse IgE (Southern Biotech) at room temperature. After rigorous washing, each well was reacted with OPD substrate solution, the reaction was terminated with 2.5N H_2SO_4, and absorbance at 490nm was determined with a microplate reader. IgE concentration (μg/mL) was determined from the standard curve of known IgE concentration.

In vivo CD4 T cell depletion, IFN-γ neutralization, and IL-17 neutralization

For CD4 T cell depletion, mice were injected with 100μg of anti-CD4 monoclonal antibody (clone GK1.5, generated at the Lymphocyte Culture Center of University of Virginia) in PBS starting at the same time as the first DT injection, then every 3 to 4 days until 3 weeks. Mice were euthanized at 8 weeks. For IFN-γ neutralization, mice were injected with 500μg of anti-IFN-γ antibody (Clone XMG1.2, BioXCell) in PBS starting at the same time as the first DT injection, then every 3 to 4 days until they were euthanized at 3 weeks. Control mice were injected with corresponding doses of polyclonal IgG from normal rat sera (Thermo Scientific). As a positive control, we used the same IFN-γ antibody to block the development of neonatal autoimmune ovarian disease (nAOD) (45). nAOD was induced by intraperitoneal injection of 100μg of a monoclonal antibody (1G2 clone) to zona pellucida 3 peptide 336–

342 on days 3 and 5 after birth (46), and anti-IFN-γ antibody was injected intraperitoneally every 3 to 4 days starting from postnatal day 3. Ovarian pathology was scored at 2 weeks of age as previously described (45). For IL-17 neutralization, mice were injected with 250μg of anti-IL-17A antibody (clone 17F3, BioXCell) in PBS starting at the same time as the first DT injection, then every 2 to 3 days until they were euthanized at 3 weeks. This dosing regime was based on previous publications (47). Control mice were injected with corresponding doses of polyclonal IgG from normal rat sera (Thermo Scientific).

Antibiotic treatment

Mice were treated with water or antibiotics beginning 7 days prior to the first dose of DT treatment and lasting for 2.5 weeks total. Mice were subjected to daily oral gavage with 200uL of autoclaved water or autoclaved water supplemented with neomycin (1mg/mL, Sigma-Aldrich), vancomycin (0.5mg/mL, Sigma-Aldrich), metronidazole (1mg/mL, Sigma-Aldrich), gentamicin (1mg/mL, Sigma-Aldrich), ampicillin (1mg/mL, Sigma-Aldrich) and filtered through a 0.2μm syringe filter, as previously described (48). WT mice treated with DT and antibiotics were used as controls. Mice were harvested 3 weeks after the first dose of DT.

Cell isolation from lymph nodes, spleen, and gastric mucosa

At euthanization, the spleen, stomach-draining lymph nodes (SDLN), non-draining axillary and brachial lymph nodes (NDLN), and/or pooled (paragastric, renal, cervical) lymph nodes were removed and prepared into single cell suspensions in RPMI Medium 1640 (Life Technologies) by mechanical disruption and filtration through a 70μm cell strainer. Splenic erythrocytes were lysed using NH_4Cl buffer. The stomach infiltrating cells were isolated as described (49). Briefly, after the stomach contents were removed by several washes in ice cold PBS, the stomach mucosa was injected with 20mL of cold PBS containing 5% FBS using a 5mL syringe and 26g needle. The stomach was gently massaged to release the infiltrating cells that were then filtered through a 70μm nylon mesh, centrifuged at 400xg for 5min, counted, and stained for flow cytometry.

Flow cytometric analysis

Single cell suspensions were stained with antibodies to CD4 (RM4-5), CD45 (30-F11), PD1 (RMP1-30), GITR (DTA-1), CD11b (M1/70), PD-L2 (CD273, 122), and ILT3 (gp49 receptor, H1.1) purchased from eBioscience and CD25 (PC61), CD69 (H1.2F3), CXCR5 (2G8), SiglecF (E50-2440), Ly6G (1A8), CD44 (IM7), CD62L (MEL-14), CD11c (HL3), and MHCII (25-9-17 and 10-3.6) purchased from BD Pharmingen. For cell surface staining, FcγRII/III were blocked with 2.4G2 antibody and cells were stained for 20min at 4°C with antibodies to the appropriate surface markers. Dead cells were excluded by Live/Dead red dead cell stain kit (Life Technologies) and samples were fixed with 2% paraformaldehyde. For intracellular staining, cells were fixed and permeabilized with the Cytofix/Cytoperm kit (BD Biosciences) or the Foxp3 Staining Kit (eBioscience) and then stained with antibodies to IRF4 (3E4, eBioscience), Foxp3 (FJK-16s, eBioscience), or CTLA-4 (UC10-4F10-11, BD Pharmingen). For intracellular cytokine staining, the isolated lymph node cells were restimulated *in vitro* with 50ng/mL PMA (Sigma-Aldrich) and 2μg/mL ionomycin (Sigma-Aldrich) at 1×10^6 cells/mL in RPMI medium 1640 (Life Technologies), supplemented with

10% (v/v) heat-inactivated FCS, (HyClone), penicillin and streptomycin (Gibco), L-glutamine (Gibco), non-essential amino acids (Gibco), sodium pyruvate (Gibco), HEPES (Gibco), and 2-ME (Sigma-Aldrich). After 2h, 10μg/mL of brefeldin A (BD Biosciences) was added and 4h later, the cells were stained with anti-CD4 antibody. The cells were then fixed and permeabilized using the Cytofix/Cytoperm kit (BD Biosciences) and stained for intracellular IL-4 (11B11, eBioscience), IL-5 (TRFK5, BD Pharmingen), IFN-γ (XMG1.2, BD Pharmingen), or IL-17 (ebioTC11-18H10.1, eBioscience). Flow cytometry data were acquired on a five-color FACSscan or six-color FACSCanto I flow cytometer (BD Biosciences) using BD FACS Diva Software (Version 6.0) and analyzed with FlowJo software (Tree Star).

In vitro CD4+CD25+ Treg cell suppression assay

4×10^5/mL CD4+CD25− naïve T cells were purified from the lymph nodes of untreated WT mice using CD4+CD25+ MicroBeads (Miltenyi Biotec) and AutoMACS (Miltenyi Biotec) according to the manufacturer's instructions. They were cultured with graded numbers of CD4+CD25+ Treg cells isolated from the lymph nodes of naïve or Treg cell-depleted DEREG mice. Alternatively, 4×10^5/mL CD4+CD25− T cells were purified from the lymph nodes of WT mice or Treg cell-depleted DEREG mice and were cultured with graded numbers of CD4+CD25+ Treg cells isolated from the pooled lymph nodes of untreated WT mice. The purity of the isolated CD4+CD25+ cells was 91.4±5.1%. In each experiment, cell mixtures were cultured in the presence of 4×10^6/mL irradiated splenocytes as antigen presenting cells and anti-CD3 monoclonal antibody diluted 1:1000 (Cedarlane) in a 96-well round-bottom plate for 80h. Cell proliferation was assessed by [3H]thymidine incorporation during the final 8h of culture. Percentage of suppression was calculated as described previously (50).

In vivo Treg cell reconstitution

CD4+CD25+ Treg cells were isolated from pooled lymph nodes and spleens of WT donors. Erythrocyte lysed spleen cells were enriched for the T cell fraction on a mouse T cell enrichment column (R&D Systems). CD4+CD25− T cells were isolated using CD4+CD25+ Microbeads (Miltenyi Biotec) and AutoMACS (Miltenyi Biotec). Treg cell-depleted B6AF1-DEREG mice were injected intravenously with 2×10^6 viable Treg cells, either at the time of the first dose of DT treatment or 7 days later. The purity of the isolated CD4+CD25+ cells was 97.5±2.2%.

Statistical analyses

Statistical differences were determined by the unpaired Mann-Whitney test, Kruskel-Wallis test with Dunns posttests, or Spearman correlation test using GraphPad Prism Version 5.0. The one-tailed fisher exact test was used to assess differences in disease incidences. Analyses of *in vitro* suppression assays were performed after transforming the percent suppression data to the log10 scale. Three-way analysis of variance (ANOVA) was used, with the experiment factor taken as a random effect. F-tests were used to compare differences between groups. A p value of <0.05 was considered statistically significant.

Results

CD4+ T cell-dependent autoimmune gastritis occurs in DEREG mice following CD4+Foxp3+ Treg cell depletion

To address the role of Treg cells in physiological self-tolerance, we investigated the emergence of spontaneous autoimmune diseases in adult mice with Treg cell depletion. Depletion of ~60% of Treg cells in WT C57BL/6 or (C57BL/6 x A/J)F$_1$ (B6AF1) mice by anti-CD25 antibody (PC61) treatment did not result in autoimmune disease (51, 52). However, autoimmune gastritis was observed in adult DEREG mice after about 90% of Treg cells were ablated by three DT injections (days 0, 2, and 5). A complete autopsy revealed severe autoimmune immunopathology in the stomach of Treg cell-depleted C57BL/6-DEREG and B6AF1-DEREG mice; they had comparable disease incidences and severity and showed no gender bias (Supplemental Figure 1A, B). Mild and focal monocytic inflammatory infiltrates were observed in the kidney, pancreas, liver, salivary gland, lung, and lacrimal gland of some Treg cell-depleted mice, whereas the eye, skin, small bowel, and large bowel were devoid of inflammation (data not shown).

Inflammatory cell infiltration appeared in the gastric mucosa of DT-treated DEREG mice by 1 week after the first dose of DT treatment. Disease incidence was significantly elevated by week 2 (p=0.0303) (Figure 1B). By 3–4 weeks, there was significant escalation of the severity gastric inflammation, loss of parietal cells, mucosal epithelial cell hyperplasia with mucinous metaplasia, and hypertrophy of the mucosa and muscularis externa (Figure 1A, B). Maximal AIG was found in the gastric wall of the proximal stomach and extended to the squamous epithelium of the adjacent cardia (the mouse "abdominal" esophagus), but spared the gastric antrum and the thoracic esophagus (data not shown). Notably, severe AIG persisted for at least 16 weeks after Treg cell depletion (Figure 1B). These pathological changes account for the increased stomach weight (Figure 1C), providing a quantitative assessment of the overall AIG pathology that correlates with the gastritis severity (Figure 1D). We observed no difference in the stomach weights between the C57BL/6-DEREG and B6AF1-DEREG mice (Supplemental Figure 1C). The control DEREG mice treated with PBS showed no evidence of AIG (Figure 1A–C). Moreover, gastric inflammation was not due to DT toxicity or off-target expression of the DTR transgene, because the stomachs of DT-treated WT mice (Figure 1A–C) and DT-treated Rag1$^{-/-}$ DEREG mice were free of pathology (n=7; data not shown).

Treg cell depleted DEREG mice exhibited an increase in CD4+Foxp3− T cells numbers in the pooled lymph nodes (Figure 1E). Their activation status was evident by an increase in percentages and numbers of CD69+ CD4+Foxp3− cells at 2 weeks after Treg cell depletion (Figure 1F), and by an elevation of CD44^{hi}CD62L^{lo} effector/memory CD4+Foxp3− T cell frequency and numbers at 3 weeks, most pronounced in the stomach-draining lymph nodes (SDLN) (Figure 1G). To investigate the pathogenic role of the activated CD4+Foxp3− T cells in AIG, we depleted CD4+ cells by injecting a monoclonal anti-CD4 antibody for 3 weeks starting at the time of the first dose of DT. This resulted in a significant reduction of gastritis at 8 weeks (Figure 1H). The robust gastric autoantibody response detected in DEREG mice with AIG was also significantly reduced after CD4+ T cell depletion (Figure

1H). Together, our findings indicate that Treg cell depletion alone results in severe CD4+ T cell-dependent AIG in DEREG mice.

DEREG mice with AIG develop serum autoantibodies to the gastric parietal cell H +K⁺ATPase and intrinsic factor (IF)

Dysregulation of T follicular helper (Tfh) cells is associated with development of autoimmunity through the promotion of autoantibody production (53). In support of the gastric autoantibody response (Figure 1F), we observed a significant expansion of PD1+CXCR5+ Tfh cells in the SDLN at 3 weeks (Figure 2A). We also observed a concomitant increase in the absolute numbers of Tfh cells in the NDLN (Figure 2A), likely due to the increased total lymph node cellularity after Treg cell depletion (data not shown).

Treg cell-depleted DEREG mice developed autoantibodies to gastric antigens located in the basal epithelial cells as well as the parietal cells. Of the antibody-positive mice at 3 weeks, 31% reacted with parietal cells only (Figure 2B), 28% reacted with basal gland epithelial cells only (Figure 2C), and 41% reacted with both (Figure 2D). At 8 weeks, 58% of the autoantibodies reacted with both parietal cells and basal gland epithelial cells, while 37% or 5% reacted with parietal cells or basal gland epithelial cells alone, respectively. Serum autoantibodies were detected by week 2 and persisted through week 16 (Figure 2E). Autoantibodies against gastric H⁺K⁺ATPase were detected in 82% of Treg cell-depleted mice by 5–6 weeks (Figure 2F).

We next investigated the specificity of the autoantibodies to the basal gland epithelial cells. Specifically, we addressed whether they targeted IF expressed primarily in murine gastric chief cells (54). Autoantibodies to IF are common in human AIG (55–57), yet were not detected in some experimental AIG models (58). To address this, we first co-stained normal stomach sections with sera from Treg cell-depleted mice with AIG and goat anti-human IF antibody. They reacted with antigens present in the same cytoplasmic locations within the basal epithelial cells (Figure 2G), especially in vesicular structures with a punctate distribution (Figure 2G inset). We then developed an ELISA to detect IF autoantibodies and found that about 50% of mice with AIG and serum basal epithelial cell autoantibodies targeted IF (Figure 2H).

These findings indicate that Tfh cell responses and autoantibody production to both gastric H⁺K⁺ATPase and IF are normally controlled by Treg cells in mice, and autoantibody responses to both antigens can occur spontaneously in mice with AIG following Treg cell depletion. The presence of these autoantibodies is consistent with the clinical observations in patients with AIG (20).

After DT-mediated Treg cell depletion, the Treg cells rapidly rebound and exhibit normal tissue distribution and expression of Treg cell-associated functional molecules

After DT injection, the lymph node CD4+Foxp3+ Treg cells rebounded within 14 – 21 days (Supplemental Figure 2A). Nonetheless, AIG developed and progressed (Figure 1) despite the return of Treg cells to normal frequencies. This was not due to a major homing defect of the rebounded Treg cells, because a normal frequency and absolute number of Foxp3+CD4+ cells was detected in the SDLN, and significantly more Foxp3+CD4+ cells were found in

the stomach of DEREG mice with AIG when compared to control mice at 3 weeks (Supplemental Figure 2B, C).

We next investigated the expression levels of cytotoxic T lymphocyte associated protein-4 (CTLA-4), glucocorticoid-induced tumor necrosis factor receptor (GITR), CD25, and interferon regulatory factor 4 (IRF4) on the rebounded Treg cells compared to Treg cells from control mice. CTLA-4, a marker of Treg cell activation, is essential for their suppressive function (59–63) and for induction of Th2 cell apoptosis (64). Mice with CTLA-4-deficient Treg cells develop high titers of serum IgE and autoimmune disease in several organs, including the stomach (62). GITR and CD25 are critical for Treg cell costimulation (65) and survival (27, 66), and Treg cells with a low level of CD25 are more prone to conversion into pathogenic effector cells (67, 68). IRF4 expression has been shown to promote Treg cell homeostasis and effector functions, including suppression of Th2 responses (69, 70). Compared to control Treg cells, the rebounded Treg cells from the SDLN of DEREG mice expressed equivalent or higher, rather than lower, mean fluorescent intensities of Foxp3, CTLA-4, CD25, GITR, and IRF4 (Supplemental Figure 2D). Therefore, the rebounded Treg cells appear to retain a normal phenotype.

AIG and autoantibody responses in DT-treated DEREG mice are preventable by WT Treg cell transfer at the time of DT treatment but not at seven days after DT treatment

To further investigate AIG development despite normal Treg cell rebound, we evaluated the effect of Treg cell reconstitution on the development of the gastric autoimmune response and AIG. When WT Treg cell transfer was performed on the same day as the first DT dose, the expansion of CXCR5+PD1+ Tfh cells (Figure 3A) and activation of effector T cells (Figure 3B) were abolished in the DEREG recipients studied 3 weeks later. Moreover, the stomachs were free of inflammation and loss of parietal cells, and gastric autoantibodies were no longer detected in the serum (Figure 3C). However, when the transfer of WT Treg cells was delayed to day 7 after the first DT dose, the gastric pathology and autoantibody responses were no longer prevented at 3 weeks (Figure 3C). Therefore, within just 1 week after the initial DT treatment, the autoimmune responses in the DEREG mice were less sensitive to suppression by Treg cells.

The rebounded Treg cells exhibit normal suppressive capacity, but the effector T cells are less susceptible to Treg cell-mediated suppression *in vitro*

We next evaluated both the functional capacity of the rebounded Treg cells and the susceptibility of DEREG effector T cells to Treg cell-mediated suppression *in vitro*. We isolated the CD4+CD25+ Treg cells from DEREG mice 3 weeks after the first dose of DT and assessed their capacity to suppress the proliferation of WT CD4+CD25– effector T cells. The rebounded Treg cells from DEREG mice were just as potent as WT Treg cells in the *in vitro* suppression assay (Figure 3D, p=0.0950). Therefore, the rebounded Treg cells appeared to retain a normal suppressive function. In contrast, the CD25-CD4+ effector T cells isolated from the SDLN of mice with AIG were significantly less susceptible to suppression when compared to those from AIG-free control mice (Figure 3E, p=0.0280).

Based on these *in vitro* and *in vivo* findings, we conclude that while the rebounded Treg cells retain suppressive potential, the expanded CD4+CD25− T cells rapidly become less susceptible to Treg cell-mediated suppression. These findings further support the conclusion that the naturally-occurring Treg cells present in normal DEREG mice are responsible for maintaining physiological tolerance to gastric autoantigens.

Treg cell-depleted DEREG mice develop a Th2-dominant autoimmune response and gastric immunopathology typical of a Th2 immune response

At 1 week, when the gastric mucosa retained normal integrity, numerous eosinophils began to infiltrate the gastric submucosa and basal mucosa (Figure 4A). By 3 weeks, when parietal cell reduction was manifested, SiglecF+ eosinophils further expanded and infiltrated all layers of the stomach wall (Figure 4B). Additionally, small clusters of plasma cells were detected among the eosinophils and other mononuclear cells in the submucosa and the muscle wall (data not shown). We also observed a major restructuring of the gastric mucosa including a reduction in parietal cells, metaplasia of mucin-rich epithelial cells identified by the Periodic Acid-Schiff stain, and severe mucosal hyperplasia (Figure 4C and Figure 1A). Notably, the eosinophilic infiltration and muscular hypertrophy also affected the keratinized squamous epithelial cell lining of the adjacent gastric cardia (data not shown).

We next determined the serum gastric autoantibody isotypes as indicators of Th1 and Th2 responses; class-switch recombination to IgG1 and IgE is enhanced by IL-4, whereas class-switch recombination to IgG2a is enhanced by IFN-γ (71–73). The intensities of the IgG1 autoantibodies to parietal cells and basal epithelial cells were significantly higher than the intensities of the IgG2a autoantibodies (Figure 4D). In addition, the total serum IgE levels in the DEREG mice at 3 weeks were 11-fold greater than those of control mice (Figure 4E). The prevalence of the parietal cell and basal epithelial cell IgG1 versus IgG2a autoantibodies and total serum IgE levels were also significantly different (p <0.0001 for all comparisons).

A significant increase in the proportion of IL-4+ or IL-5+ CD4+ T cells was detected in the SDLN, with a concomitant increase in the absolute numbers of IL-4+ and IL-5+ CD4+ T cells in both the SDLN and NDLN (Figure 4F, G). We detected only minimal IL-17 production by the lymph node CD4+ T cells (Supplemental Figure 3A, B). Although IFN-γ production by lymph node CD4+ T cells was also detected (Supplemental Figure 3A, B), the severity and frequency of AIG in the Treg cell-depleted DEREG mice were not affected by treatment with an IFN-γ antibody (Supplemental Figure 3C). As a control, the same IFN-γ antibody blocked the development of neonatal autoimmune ovarian disease (Supplemental Figure 3D), which is IFN-γ-dependent (45). Furthermore, the severity and frequency of AIG in Treg cell-depleted DEREG mice was not affected by treatment with an IL-17 antibody (Supplemental Figure 3E).

These findings indicate that AIG in Treg cell-depleted DEREG mice exhibits the characteristics of a Th2 response. In the next studies, we investigated the pathogenic role of the autoimmune Th2 responses in AIG.

IL-4 and Th2 responses are critical for mediating gastric mucosal injury and eosinophilic inflammation after Treg cell depletion

IL-4 is a critical cytokine for Th2 responses (74). We therefore predicted that DEREG mice lacking IL-4 would have diminished AIG development after Treg cell depletion. The total gastric IgG1 autoantibody responses and total serum IgE levels were significantly reduced in the IL-4$^{-/-}$ DEREG mice after Treg cell depletion (Figure 5A, B), whereas the incidence and intensity of total IgG2a antibody responses were unaltered (Figure 5A).

Compared to IL-4-sufficient DEREG mice, the overall gastritis severity (Figure 5C) and stomach weights (Figure 5D) were significantly reduced in the IL-4$^{-/-}$ DEREG mice after Treg cell depletion. This reduced pathology was mainly accounted for by the reduction of parietal cell loss and mucin-rich cellular metaplasia (Figure 5E). Although the extent of gastric inflammation was unchanged (Figure 5E), the eosinophil-rich infiltrate of IL-4-sufficient DEREG mice was diminished and replaced by lymphomonocytic cells in IL-4$^{-/-}$ DEREG mice (Figure 5F, G). We did observe a slight increase in Ly6G+ neutrophils in the IL-4$^{-/-}$ DEREG mice after Treg cell depletion (Figure 5G).

These results indicate that IL-4 is a major contributor to AIG pathogenesis, including the destruction of gastric parietal cells. The reduction in mucin-rich cellular metaplasia is consistent with a role for IL-4 and Th2 responses in mucinous cell expansion observed in airway remodeling in asthma models (75–77). Because eosinophilic infiltration in the stomach was IL-4-dependent, we next investigated the role of eosinophils in AIG pathogenesis.

Eosinophils expand in the lymph nodes, support IgE responses, and exert a pathogenic effect in AIG of Treg cell-depleted mice

Eosinophils have a pathogenic role in models of allergic asthma and helminth infection (78, 79). In addition to their expansion in the stomach (Figure 4A, 4B, 5G), we also detected an increase in eosinophil percentages in the pooled lymph nodes within 2 weeks and in absolute numbers within 1 week after Treg cell depletion (Figure 6A). Notably, the eosinophils accounted for a larger fraction of the total cellularity in the SDLN and NDLN of the Treg cell-depleted DEREG mice at 3 weeks (Figure 6B). To investigate the contribution of eosinophils to AIG, we studied PHIL mice that express the diphtheria toxin A catalytic subunit under the eosinophil peroxidase promoter and are developmentally deficient in eosinophils (80). Indeed, the loss of eosinophils led to a significant reduction in the serum IgE levels of the DEREG PHIL mice (Figure 6C). In contrast, the incidence and intensity of the total IgG1 or IgG2a gastric autoantibody responses remained unchanged (Figure 6D).

At 3 weeks, the overall gastritis scores and disease incidence in the DEREG PHIL mice were significantly reduced compared to the eosinophil-sufficient DEREG mice (Figure 6E). In the absence of eosinophils, there was significant reduction in gastric inflammation and mucin-rich cellular metaplasia. There was also a trend toward reduction in parietal cell loss, although the difference did not reach statistical significance (Figure 6F, G). Gastric hypertrophy was also reduced in the mice without eosinophils (Figure 6G), accompanied by a significant reduction in the stomach weight compared to eosinophil-sufficient DEREG

mice (Figure 6H). As a control, the WT PHIL mice did not develop gastric pathology or autoantibody responses after DT treatment (data not shown). These results indicate that the eosinophilic inflammation is a significant contributor to multiple facets of AIG pathogenesis in Treg cell-depleted mice.

Intestinal microbiome alteration by oral antibiotic treatment did not affect the development of Th2-dominant AIG in Treg cell-depleted DEREG mice

A challenging question is why the DEREG mice with transient Treg cell deficiency developed a dominant pathogenic Th2 response. Environmental factors, such as the microbiome, may contribute to disease susceptibility as well as the Th2-bias in AIG of Treg cell-depleted DEREG mice. Alterations in commensal microbial communities have been found to influence Th2 responsiveness (81–83). We addressed whether the microbiome of the DEREG mice in our colony impacted disease susceptibility and Th2 bias by using an established protocol of oral antibiotic gavage to manipulate the intestinal microbiota (48). The mice responded appropriately to antibiotic treatment, as they all developed enlarged cecums and soft stool, as expected. Antibiotic-treated DEREG mice developed severe eosinophilic AIG (Supplemental Figure 4A) with increased stomach weights (Supplemental Figure 4B) at 3 weeks after DT-treatment. These results were comparable to those of water-treated DEREG mice after Treg cell depletion (Supplemental Figure 4A, B). Additionally, the IgG1-dominant gastric autoantibody production (Supplemental Figure 4C) and the IL-4 and IL-5 cytokine production by SDLN CD4+ T cells after restimulation (Supplemental Figure 4D) were similar in the water-treated and the antibiotic-treated DEREG mice after Treg cell depletion. These findings indicate that the intestinal microbiome does not promote the development of Th2-dominant AIG in our DEREG colony.

The DEREG mice with Th2-associated AIG have expanded IRF4+PD-L2+ dendritic cells and ILT3+ Treg cells

We further addressed why AIG in Treg cell-depleted mice has a Th2 bias by testing the hypothesis that the expanded dendritic cells (DCs) and the rebounded Treg cells may express molecules that have recently been shown to promote Th2 responses.

A specialized subset of DCs that express programmed death ligand 2 (PD-L2) on their cell surface and the transcription factor IRF4 have been found to regulate Th2 differentiation *in vivo* (84, 85). We observed a significant increase in total CD11c+ DCs in the pooled LN from DEREG mice by 1 week after Treg cell-depletion (Figure 7A). Indeed, among the expanded CD11c+ MHCII+ DCs, we readily detected a higher frequency and absolute number of cells co-expressing IRF4 and PD-L2 in the pooled SDLN and NDLN of Treg cell-depleted mice compared to control mice (Figure 7B, C).

In another recent study, a newly discovered population of ILT3+ Treg cells was found to promote the maturation of IRF4+PD-L2+ DCs and participate in controlling the development of Th2 cell responses *in vitro* and *in vivo* (86). Indeed, when we assessed the rebounded Treg cell population at 3 weeks, a significantly elevated percentage and absolute number of ILT3+ Treg cells were detected in the Treg cell-depleted mice compared to

control mice (Figure 7D, E). Notably, an increase in the frequency of ILT3+ Treg cells was observed in the SDLN but not the NDLN of DEREG mice.

Together, our findings suggest that an early expansion of IRF4+PD-L2+ DCs and a disequilibrium between ILT3+ and ILT3− Treg cell subsets may contribute to the Th2-dominant immune responses of Treg cell-depleted DEREG mice.

Discussion

We have shown that severe AIG occurs in C57BL/6 and B6AF1 DEREG mice after transient Treg cell depletion. AIG in these mice is characterized by dominant eosinophilic inflammation, together with parietal cell loss, mucinous metaplasia of mucosal epithelial cells, production of Th2-biased gastric autoantibodies that target both $H^+K^+ATPase$ and IF, and T cell activation and Th2 cytokine production in the regional lymph nodes. Our data indicate that these changes are the product of the rapid loss of effector T cell susceptibility to suppression by Treg cells.

Our study, along with others (40, 69) provides conclusive evidence that Treg cells are critical in maintaining physiological tolerance to murine gastric autoantigens. However, our findings differ from previous AIG studies in several important aspects. First, AIG was not observed in adult C57BL/6 or BALB/c DEREG mice after a similar regimen of Treg cell depletion (42, 44). The different outcomes could be explained by diverse environmental factors as well as differences in the microbiomes, known to influence autoimmune diseases. In this regard, our mice tested negative for pinworm and fur mite infestations known to skew toward Th2 responses (87, 88), and the AIG severity and Th2 phenotype were not altered by a standard regime of oral antibiotic treatment. Thus, the intestinal microbiota do not appear to promote the gastric-specific autoimmune responses and Th2-biased disease in our DEREG colony. However, a role for the microbiome in suppression of AIG development in other mouse colonies is a possibility that has not been investigated. Second, our study indicates that the DEREG and Foxp3-DTR knock-in mice (39) exhibit different responses and clinical outcomes after Treg cell depletion, though the nature of these differences is not fully understood. Third, similar to other AIG models induced by immunization (89) or d3tx (34), the rebounded Treg cells in our model are functional. However, no immunization boost or lymphopenia is required in Treg cell-depleted DEREG mice for the effector T cell to resist Treg cell-mediated suppression.

The current paradigm posits that autoimmune diseases are dependent on Th1 or Th17 responses and less reliant on Th2 responses, and this applies to studies on AIG (31, 90–92). Th2 cells are generally regarded as counter-inflammatory to Th1-dominant autoimmunity with therapeutic potential (93–96). However, pathogenic Th2 responses in autoimmunity have also been suggested by previous studies. For example, studies on AIG have documented activated Th1 and Th2 autoantigen-specific T cells in the regional lymph nodes of d3tx mice. Both the $H^+K^+ATPase$-specific Th1 and Th2 cell clones can transfer severe AIG (32) and TCR transgenic mice generated from these T cell clones spontaneously develop AIG (97, 98). Additionally, naïve transgenic T cells were able to transfer disease to immunodeficient recipients after *in vitro* differentiation to Th1, Th2, and Th17 cells (91).

Disease transfer by Th2 cells has also been documented in several other autoimmune diseases (99–102). In this study, we have provided clear evidence for the spontaneous occurrence of a pathogenic Th2 response after Treg cell depletion alone, without the requirement for adjuvant, lymphopenia, or use of a transgenic TCR. Our findings will likely have clinical relevance because, despite limited data on human AIG, recent studies also support a possible role for Th2 responses. Bettington, *et al.* reported an increased eosinophil count in biopsies of patients with AIG (103), and Bedeir, *et al.* detected numerous IgG4-positive plasma B cells in biopsies of AIG patients with pernicious anemia (104). The latter is notable because human IgG4 production is associated with Th2 responses (105–107). While it is possible that different individual AIG patients may exhibit different combinations of helper T cell responses, our model seems appropriate for delineating a component of AIG in some patients.

Although autoantibodies to gastric H^+K^+ATPase are well defined (13), this study also provides documentation of autoantibody responses to the gastric IF in experimental AIG. Autoantibodies to IF and H^+K^+ATPase are involved in the complications of chronic atrophic gastritis and are useful diagnostic markers of AIG (21). For example, immune-mediated depletion of parietal cells can lead to hypochlorhydria, and autoantibodies to IF, by impairing the absorption of vitamin B12, can lead to pernicious anemia (108). Patients with AIG and pernicious anemia are reported to have an increased risk of developing gastric cancer (16–18). Investigation of these important sequelae of AIG is not possible with the current models of AIG due to Treg cell depletion. In this regard, the longevity of AIG in the DEREG mice and their survival after Treg cell depletion may provide an opportunity for investigation of these sequelae.

The evidence for a Th2-type of immune response in the pathogenesis of AIG is supported by the following findings: 1) the subclass of the autoantibody response, 2) the inflammatory cell infiltrate and epithelial cell response, and 3) the cytokine production. The pathogenicity of the Th2 response is supported by the significant reduction in stomach pathology and immune responses in IL-4$^{-/-}$ mice and eosinophil deficient mice. Strikingly, the phenotypes of these mice are not identical. The decreased pathology in Treg cell-depleted IL-4$^{-/-}$ mice was mainly attributed to the reduced parietal cell loss and mucin cell hyperplasia. These changes correlated with a reduced infiltration of eosinophils in the inflamed stomach. However, the degree of inflammation remained comparable to that observed in IL-4-sufficient DEREG mice, suggesting that additional mechanisms are responsible for the residual gastritis in the absence of IL-4. Although a predominant mononuclear cell infiltrate, characteristic of Th1 responses, was observed in Treg cell-depleted IL-4$^{-/-}$ mice, IFN-γ antibody treatment did not prevent AIG in these mice (data not shown) or in IL-4-sufficient DEREG mice. Also, neutrophil infiltration was scarce in Treg cell-depleted mice and treatment with IL-17 antibody did not inhibit AIG, arguing against a predominant role for Th17 responses. Thus, IL-4-dependent mechanisms appear to be major contributors to AIG in Treg cell-depleted DEREG mice.

A more dramatic reduction of gastric inflammation was observed in the Treg cell-depleted eosinophil deficient PHIL mice. In addition, there was a significant reduction in mucinous metaplasia. The major loss of parietal cells in mice with eosinophils raises the possibility

that eosinophils could have a cytotoxic role in AIG in DEREG mice. It is known that upon activation, eosinophils can release proteases and other granule mediators and exhibit strong cytotoxic effects (109). Activated eosinophils also secrete proinflammatory cytokines and chemokines that attract other pathogenic immune cells to the site of tissues injury (109, 110).

In addition to their potential roles in the efferent phase of the autoimmune response, eosinophils may also support the induction of antigen-specific Th2 cell-dependent antibody responses in the lymph nodes. In allergy models, eosinophils infiltrate the T cell zones, where they can directly present antigens to T cells or/and release cytokines that influence Th2 differentiation and Ig class switching, directly or through dendritic cells (111, 112). In the DEREG mice, Treg cell depletion also led to a rapid expansion of eosinophils in the lymph nodes, and Treg cell-depleted eosinophil deficient PHIL mice had a significant reduction in the levels of serum IgE. However, the precise meaning of this finding and the precise role for eosinophils in promoting AIG pathogenesis will require additional studies.

Why does Treg cell depletion in the DEREG mice lead to a dominant Th2 response? This could be explained by a higher Th2 cell-susceptibility to apoptosis in the presence of Treg cells, and thus, a tighter Treg cell control of Th2 cells compared to Th1 cells (64). Notably, scurfy mice and IPEX patients both develop hyper-IgE syndrome and eosinophilia. A dominant Th2 response was also observed in Foxp3-deficient mice (69) and in mice with Treg cell-specific deletion of CTLA-4 (62), ITCH (113), IRF4 (69), CK2 (86), or Nr4a (114), suggesting that these molecules expressed on Treg cells are involved in the control of Th2 responses. However, the mechanisms that link the loss of Treg cell function to the allergic Th2-type responses are not fully understood (115–119). It is possible that factors and cytokines operating locally in the stomach also influence the expression of a Th2-dominant tissue response. For example, Buzzelli *et al.* showed that IL-33 promoted a type 2 gastric inflammatory response in WT mice that resembles the AIG in DEREG mice (120).

To investigate why the DEREG mice with transient Treg cell depletion develop a dominant pathogenic Th2 response, we investigated the altered expression of certain key molecules on Treg cells and DCs that can influence the preferential induction of Th2 responses. Despite the development of uncontrolled Th2 responses in the Treg cell-depleted DEREG mice, the rebounded Treg cells did not show altered expression of Foxp3, GITR, CD25, CTLA-4 or IRF4. Two reports have demonstrated that the initiation of Th2 cell-driven immune responses depends on IRF4 expression in DCs, which controls the maturation of a PD-L2+ DC subset (84, 85). It was shown that IRF4 promotes IL-33 and IL-10 expression by DCs that induces the differentiation of Th2 cells *in vivo*. Consistent with previous reports (39), we also observed a rapid expansion of DCs after Treg cell depletion in DEREG mice. Furthermore, we detected a significant increase in the proportion and absolute numbers of IRF4+PD-L2+ DCs in the DEREG mice as early as one week after Treg cell depletion. This finding supports the hypothesis that the early expansion of a unique DC population may preferentially drive the development and activation of Th2 cells in AIG. In addition, we also found that a greater proportion and number of the rebounded Treg cells in DT-treated DEREG mice express ILT3. This is an intriguing finding because a recent study reported that ILT3 expression on Treg cells is controlled by the casein kinase 2, and the ILT3+ Treg

cells could promote the expansion of IRF4+PD-L2+ DCs (86). It is tempting to speculate, as a potential mechanism, that the Th2-dominant immune responses in the Treg cell-depleted DEREG mice may result from the cooperation of the IRF4+PD-L2+ DCs and the ILT3+ rebounded Treg cell subsets.

It is striking that a very short period of Treg cell deficiency was sufficient to allow for AIG development. Our analysis indicates that the suppressive function of the rebounded Treg cells does not appear to be compromised. Thus, the rebounded Treg cells suppress as efficiently as control Treg cells *in vitro*. In contrast, we observed that the effector T cells were less sensitive than naïve cells to Treg cell-mediated suppression within 1 week of the first dose of DT treatment. Although this state of resistance to suppression by Treg cells may be due to potential changes in the innate or adaptive immune compartments, findings from our *in vitro* studies suggest the alteration is also intrinsic to the effector T cells.

Effector T cells can resist Treg cell-mediated suppression through multiple ways. For example, the cytokine and growth factor composition in the environment, alterations in T cell receptor signaling, the anatomical location, and the number and activation status of the effector T cells can all impact the mechanism and the degree of Treg cell-mediated suppression (121, 122). Resistance to suppression has been reported in other animal models of autoimmunity and in human autoimmunity (123–131). While numerous signaling pathways can account for the resistance phenotype (122), one relevant to Th2 cell resistance might involve IL-4 signaling and STAT6 activation, as previously documented *in vitro* (132) and *in vivo* (133). Whether this lack of susceptibility to Treg cell-mediated suppression is also associated with the preferential reduction of other Treg cell subsets that regulate Th2 cells (86, 113, 114), the absence of gastric antigen-specific Treg cells among the rebounded Treg cells (34, 134), or additional possibilities (135) remains to be elucidated.

In summary, our study has shown that Th2 responses are involved in AIG, indicating that Th2 responses can participate in the pathogenesis of organ-specific autoimmune diseases in mice with transient Treg cell depletion. This is associated with the finding that the effector T cells are less sensitive to Treg cell-mediated suppression after a short period of Treg cell deficiency. These findings suggest that Treg cell therapy or the blockade of certain effector targets might not be as effective in the treatment of AIG and highlight the need for a better understanding of the crosstalk between the effector and regulatory mechanisms of T cell responses. For AIG, successful therapy may require dampening of the effector autoimmune response while strengthening the regulatory components.

Supplementary Material

Refer to Web version on PubMed Central for supplementary material.

Acknowledgments

statistical guidance, and the Research Histology Core, the Advanced Microscopy Facility, and the Lymphocyte Culture Center at the University of Virginia for their expert services.

Abbreviations used in this article

AIG	Autoimmune Gastritis
DCs	dendritic cells
DT	diphtheria toxin
GITR	glucocorticoid-induced tumor necrosis factor receptor
IF	intrinsic factor
NDLN	non-draining lymph nodes
MFI	mean fluorescence intensity
SDLN	stomach-draining lymph nodes
Tfh	T follicular helper

References

1. Xing Y, Hogquist KA. T-cell tolerance: central and peripheral. Cold Spring Harb Perspect Biol. 2012; 4:a006957. [PubMed: 22661634]

2. Sakaguchi S. Naturally arising CD4+ regulatory t cells for immunologic self-tolerance and negative control of immune responses. Annu Rev Immunol. 2004; 22:531–62. [PubMed: 15032588]

3. Hori S, Nomura T, Sakaguchi S. Control of regulatory T cell development by the transcription factor Foxp3. Science. 2003; 299:1057–61. [PubMed: 12522256]

4. Fontenot JD, Gavin MA, Rudensky AY. Foxp3 programs the development and function of CD4+CD25+ regulatory T cells. Nat Immunol. 2003; 4:330–6. [PubMed: 12612578]

5. Wan YY, Flavell RA. Regulatory T-cell functions are subverted and converted owing to attenuated Foxp3 expression. Nature. 2007; 445:766–70. [PubMed: 17220876]

6. Brunkow ME, Jeffery EW, Hjerrild KA, Paeper B, Clark LB, Yasayko SA, Wilkinson JE, Galas D, Ziegler SF, Ramsdell F. Disruption of a new forkhead/winged-helix protein, scurfin, results in the fatal lymphoproliferative disorder of the scurfy mouse. Nat Genet. 2001; 27:68–73. [PubMed: 11138001]

7. Khattri R, Cox T, Yasayko SA, Ramsdell F. An essential role for Scurfin in CD4+CD25+ T regulatory cells. Nat Immunol. 2003; 4:337–42. [PubMed: 12612581]

8. Bennett CL, Christie J, Ramsdell F, Brunkow ME, Ferguson PJ, Whitesell L, Kelly TE, Saulsbury FT, Chance PF, Ochs HD. The immune dysregulation, polyendocrinopathy, enteropathy, X-linked syndrome (IPEX) is caused by mutations of FOXP3. Nat Genet. 2001; 27:20–1. [PubMed: 11137993]

9. Torgerson TR, Ochs HD. Immune dysregulation, polyendocrinopathy, enteropathy, X-linked: forkhead box protein 3 mutations and lack of regulatory T cells. J Allergy Clin Immunol. 2007; 120:744–50. quiz 751–2. [PubMed: 17931557]

10. Jeffries GH, Hoskins DW, Sleisenger MH. Antibody to intrinsic factor in serum from patients with pernicious anemia. J Clin Invest. 1962; 41:1106–15. [PubMed: 14451527]

11. Irvine WJ, Davies SH, Teitelbaum S, Delamore IW, Williams AW. The clinical and pathological significance of gastric parietal cell antibody. Ann N Y Acad Sci. 1965; 124:657–91. [PubMed: 5320501]

12. Karlsson FA, Burman P, Lööf L, Mårdh S. Major parietal cell antigen in autoimmune gastritis with pernicious anemia is the acid-producing H+, K+-adenosine triphosphatase of the stomach. J Clin Invest. 1988; 81:475–9. [PubMed: 2828428]

13. Goldkorn I, Gleeson PA, Toh BH. Gastric parietal cell antigens of 60–90, 92, and 100–120 kDa associated with autoimmune gastritis and pernicious anemia. Role of N-glycans in the structure and antigenicity of the 60–90-kDa component. J Biol Chem. 1989; 264:18768–74. [PubMed: 2478551]

14. Toh BH, Gleeson PA, Simpson RJ, Moritz RL, Callaghan JM, Goldkorn I, Jones CM, Martinelli TM, Mu FT, Humphris DC. The 60- to 90-kDa parietal cell autoantigen associated with autoimmune gastritis is a beta subunit of the gastric H+/K(+)-ATPase (proton pump). Proc Natl Acad Sci U S A. 1990; 87:6418–22. [PubMed: 1974721]

15. Jones CM, Toh BH, Pettitt JM, Martinelli TM, Humphris DC, Callaghan JM, Goldkorn I, Mu FT, Gleeson PA. Monoclonal antibodies specific for the core protein of the beta-subunit of the gastric proton pump (H+/K+ ATPase). An autoantigen targetted in pernicious anaemia. Eur J Biochem. 1991; 197:49–59. [PubMed: 1707813]

16. Borch K, Renvall H, Liedberg G. Gastric endocrine cell hyperplasia and carcinoid tumors in pernicious anemia. Gastroenterology. 1985; 88:638–48. [PubMed: 2578420]

17. Armbrecht U, Stockbrugger RW, Rode J, Menon GG, Cotton PB. Development of gastric dysplasia in pernicious anaemia: a clinical and endoscopic follow up study of 80 patients. Gut. 1990; 31:1105–1109. [PubMed: 2083855]

18. Kokkola A, Sjöblom SM, Haapiainen R, Sipponen P, Puolakkainen P, Järvinen H. The risk of gastric carcinoma and carcinoid tumours in patients with pernicious anaemia. A prospective follow-up study. Scand J Gastroenterol. 1998; 33:88–92. [PubMed: 9489914]

19. Carmel R. Prevalence of undiagnosed pernicious anemia in the elderly. Arch Intern Med. 1996; 156:1097–100. [PubMed: 8638997]

20. Toh BH I, van Driel R, Gleeson PA. Pernicious anemia. N Engl J Med. 1997; 337:1441–8. [PubMed: 9358143]

21. van Driel, IR.; Tu, E.; Gleeson, PA. The Autoimmune Diseases. In: Rose, NR.; Machay, IR., editors. The Autoimmune Diseases. 5. Academic Press; 2014. p. 619-631.

22. Kojima A, Prehn RT. Genetic susceptibility to post-thymectomy autoimmune diseases in mice. Immunogenetics. 1981; 14:15–27. [PubMed: 7035348]

23. Sakaguchi S. Organ-specific autoimmune diseases induced in mice by elimination of T cell subset. I. Evidence for the active participation of T cells in natural self-tolerance; deficit of a T cell subset as a possible cause of autoimmune disease. J Exp Med. 1985; 161:72–87. [PubMed: 3871469]

24. Fukuma K, Sakaguchi S, Kuribayashi K, Chen WL, Morishita R, Sekita K, Uchino H, Masuda T. Immunologic and clinical studies on murine experimental autoimmune gastritis induced by neonatal thymectomy. Gastroenterology. 1988; 94:274–83. [PubMed: 3335307]

25. Tung KS. Mechanism of self-tolerance and events leading to autoimmune disease and autoantibody response. Clin Immunol Immunopathol. 1994; 73:275–82. [PubMed: 7955555]

26. Asano M, Toda M, Sakaguchi N, Sakaguchi S. Autoimmune disease as a consequence of developmental abnormality of a T cell subpopulation. J Exp Med. 1996; 184:387–96. [PubMed: 8760792]

27. Sakaguchi S, Sakaguchi N, Asano M, Itoh M, Toda M. Immunologic self-tolerance maintained by activated T cells expressing IL-2 receptor alpha-chains (CD25). Breakdown of a single mechanism of self-tolerance causes various autoimmune diseases. J Immunol. 1995; 155:1151–64. [PubMed: 7636184]

28. Sakaguchi S, Toda M, Asano M, Itoh M, Morse SS, Sakaguchi N. T cell-mediated maintenance of natural self-tolerance: its breakdown as a possible cause of various autoimmune diseases. J Autoimmun. 1996; 9:211–20. [PubMed: 8738965]

29. Itoh M, Takahashi T, Sakaguchi N, Kuniyasu Y, Shimizu J, Otsuka F, Sakaguchi S. Thymus and autoimmunity: production of CD25+CD4+ naturally anergic and suppressive T cells as a key function of the thymus in maintaining immunologic self-tolerance. J Immunol. 1999; 162:5317–26. [PubMed: 10228007]

30. Tung KS, Smith S, Teuscher C, Cook C, Anderson RE. Murine autoimmune oophoritis, epididymoorchitis, and gastritis induced by day 3 thymectomy. Immunopathology. Am J Pathol. 1987; 126:293–302. [PubMed: 3548402]

31. DiPaolo RJ, Glass DD, Bijwaard KE, Shevach EM. CD4+CD25+ T cells prevent the development of organ-specific autoimmune disease by inhibiting the differentiation of autoreactive effector T cells. J Immunol. 2005; 175:7135–42. [PubMed: 16301616]

32. Suri-Payer E, Amar AZ, McHugh R, Natarajan K, Margulies DH, Shevach EM. Post-thymectomy autoimmune gastritis: fine specificity and pathogenicity of anti-H/K ATPase-reactive T cells. Eur J Immunol. 1999; 29:669–77. [PubMed: 10064084]

33. Dujardin HC, Burlen-Defranoux O, Boucontet L, Vieira P, Cumano A, Bandeira A. Regulatory potential and control of Foxp3 expression in newborn CD4+ T cells. Proc Natl Acad Sci U S A. 2004; 101:14473–8. [PubMed: 15452347]

34. Samy ET, Wheeler KM, Roper RJ, Teuscher C, Tung KSK. Cutting edge: Autoimmune disease in day 3 thymectomized mice is actively controlled by endogenous disease-specific regulatory T cells. J Immunol. 2008; 180:4366–70. [PubMed: 18354156]

35. Wheeler KM, Samy ET, Tung KSK. Cutting edge: normal regional lymph node enrichment of antigen-specific regulatory T cells with autoimmune disease-suppressive capacity. J Immunol. 2009; 183:7635–8. [PubMed: 19923458]

36. Gleeson PA, Toh BH, van Driel IR. Organ-specific autoimmunity induced by lymphopenia. Immunol Rev. 1996; 149:97–125. [PubMed: 9005222]

37. Monteiro JP, Farache J, Mercadante AC, Mignaco JA, Bonamino M, Bonomo A. Pathogenic effector T cell enrichment overcomes regulatory T cell control and generates autoimmune gastritis. J Immunol. 2008; 181:5895–903. [PubMed: 18941178]

38. Datta S, Sarvetnick N. Lymphocyte proliferation in immune-mediated diseases. Trends Immunol. 2009; 30:430–8. [PubMed: 19699149]

39. Kim JM, Rasmussen JP, Rudensky AY. Regulatory T cells prevent catastrophic autoimmunity throughout the lifespan of mice. Nat Immunol. 2007; 8:191–7. [PubMed: 17136045]

40. Nyström SN, Bourges D, Garry S, Ross EM, van Driel IR, Gleeson PA. Transient Treg-cell depletion in adult mice results in persistent self-reactive CD4(+) T-cell responses. Eur J Immunol. 2014; 44:3621–31. [PubMed: 25231532]

41. Teh CE, Gray DHD. Can you rely on Treg cells on the rebound? Eur J Immunol. 2014; 44:3504–7. [PubMed: 25410151]

42. Lahl K, Loddenkemper C, Drouin C, Freyer J, Arnason J, Eberl G, Hamann A, Wagner H, Huehn J, Sparwasser T. Selective depletion of Foxp3+ regulatory T cells induces a scurfy-like disease. J Exp Med. 2007; 204:57–63. [PubMed: 17200412]

43. Mayer CT, Ghorbani P, Kühl AA, Stüve P, Hegemann M, Berod L, Gershwin ME, Sparwasser T. Few Foxp3(+) regulatory T cells are sufficient to protect adult mice from lethal autoimmunity. Eur J Immunol. 2014; 44:2990–3002. [PubMed: 25042334]

44. Berod L, Stüve P, Varela F, Behrends J, Swallow M, Kruse F, Krull F, Ghorbani P, Mayer CT, Hölscher C, Sparwasser T. Rapid rebound of the Treg compartment in DEREG mice limits the impact of Treg depletion on mycobacterial burden, but prevents autoimmunity. PLoS One. 2014; 9:e102804. [PubMed: 25050936]

45. Setiady YY, Pramoonjago P, Tung KSK. Requirements of NK cells and proinflammatory cytokines in T cell-dependent neonatal autoimmune ovarian disease triggered by immune complex. J Immunol. 2004; 173:1051–8. [PubMed: 15240693]

46. Rival C, Samy E, Setiady Y, Tung K. Cutting edge: Ly49C/I⁻ neonatal NK cells predispose newborns to autoimmune ovarian disease induced by maternal autoantibody. J Immunol. 2013; 191:2865–9. [PubMed: 23960238]

47. Russell SE, Stefanska AM, Kubica M, Horan RM, Mantovani A, Garlanda C, Fallon PG, Walsh PT. Toll IL-1R8/single Ig IL-1-related receptor regulates psoriasiform inflammation through direct inhibition of innate IL-17A expression by γδ T cells. J Immunol. 2013; 191:3337–46. [PubMed: 23945140]

48. Hill DA, Hoffmann C, Abt MC, Du Y, Kobuley D, Kirn TJ, Bushman FD, Artis D. Metagenomic analyses reveal antibiotic-induced temporal and spatial changes in intestinal microbiota with

associated alterations in immune cell homeostasis. Mucosal Immunol. 2010; 3:148–58. [PubMed: 19940845]

49. Alderuccio F, Toh BH, Gleeson PA, van Driel IR. A novel method for isolating mononuclear cells from the stomachs of mice with experimental autoimmune gastritis. Autoimmunity. 1995; 21:215–21. [PubMed: 8822279]

50. Collison LW, Vignali DAA. In vitro Treg suppression assays. Methods Mol Biol. 2011; 707:21–37. [PubMed: 21287326]

51. McHugh RS, Shevach EM. Cutting Edge: Depletion of CD4+CD25+ Regulatory T Cells Is Necessary, But Not Sufficient, for Induction of Organ-Specific Autoimmune Disease. J Immunol. 2002; 168:5979–5983. [PubMed: 12055202]

52. Wheeler K, Tardif S, Rival C, Luu B, Bui E, Del Rio R, Teuscher C, Sparwasser T, Hardy D, Tung KSK. Regulatory T cells control tolerogenic versus autoimmune response to sperm in vasectomy. Proc Natl Acad Sci U S A. 2011; 108:7511–6. [PubMed: 21502500]

53. Zhang X, Ing S, Fraser A, Chen M, Khan O, Zakem J, Davis W, Quinet R. Follicular helper T cells: new insights into mechanisms of autoimmune diseases. Ochsner J. 2013; 13:131–9. [PubMed: 23531878]

54. Lorenz RG, Gordon JI. Use of transgenic mice to study regulation of gene expression in the parietal cell lineage of gastric units. J Biol Chem. 1993; 268:26559–70. [PubMed: 8253786]

55. Ungar B, Whittingham S, Francis CM. Pernicious anaemia: incidence and significance of circulating antibodies to intrinsic factor and to parietal cells. Australas Ann Med. 1967; 16:226–9. [PubMed: 4861883]

56. Carmel R. Reassessment of the relative prevalences of antibodies to gastric parietal cell and to intrinsic factor in patients with pernicious anaemia: influence of patient age and race. Clin Exp Immunol. 1992; 89:74–7. [PubMed: 1628426]

57. Davidson RJ, Atrah HI, Sewell HF. Longitudinal study of circulating gastric antibodies in pernicious anaemia. J Clin Pathol. 1989; 42:1092–5. [PubMed: 2584410]

58. Greenwood DLV, Sentry JW. Murine experimental autoimmune gastritis models refractive to development of intrinsic factor autoantibodies, cobalamin deficiency and pernicious anemia. Clin Immunol. 2007; 122:41–52. [PubMed: 17035094]

59. Waterhouse P, Penninger JM, Timms E, Wakeham A, Shahinian A, Lee KP, Thompson CB, Griesser H, Mak TW. Lymphoproliferative disorders with early lethality in mice deficient in Ctla-4. Science. 1995; 270:985–8. [PubMed: 7481803]

60. Tivol EA, Borriello F, Schweitzer AN, Lynch WP, Bluestone JA, Sharpe AH. Loss of CTLA-4 leads to massive lymphoproliferation and fatal multiorgan tissue destruction, revealing a critical negative regulatory role of CTLA-4. Immunity. 1995; 3:541–7. [PubMed: 7584144]

61. Bour-Jordan H, Grogan JL, Tang Q, Auger JA, Locksley RM, Bluestone JA. CTLA-4 regulates the requirement for cytokine-induced signals in T(H)2 lineage commitment. Nat Immunol. 2003; 4:182–8. [PubMed: 12524538]

62. Wing K, Onishi Y, Prieto-Martin P, Yamaguchi T, Miyara M, Fehervari Z, Nomura T, Sakaguchi S. CTLA-4 control over Foxp3+ regulatory T cell function. Science. 2008; 322:271–5. [PubMed: 18845758]

63. Walker LSK. Treg and CTLA-4: two intertwining pathways to immune tolerance. J Autoimmun. 2013; 45:49–57. [PubMed: 23849743]

64. Tian L, Altin JA, Makaroff LE, Franckaert D, Cook MC, Goodnow CC, Dooley J, Liston A. Foxp3$^+$ regulatory T cells exert asymmetric control over murine helper responses by inducing Th2 cell apoptosis. Blood. 2011; 118:1845–53. [PubMed: 21715314]

65. Ono M, Shimizu J, Miyachi Y, Sakaguchi S. Control of autoimmune myocarditis and multiorgan inflammation by glucocorticoid-induced TNF receptor family-related protein(high), Foxp3-expressing CD25+ and CD25– regulatory T cells. J Immunol. 2006; 176:4748–56. [PubMed: 16585568]

66. Fontenot JD, Rasmussen JP, Gavin MA, Rudensky AY. A function for interleukin 2 in Foxp3-expressing regulatory T cells. Nat Immunol. 2005; 6:1142–51. [PubMed: 16227984]

67. Komatsu N, Mariotti-Ferrandiz ME, Wang Y, Malissen B, Waldmann H, Hori S. Heterogeneity of natural Foxp3+ T cells: a committed regulatory T-cell lineage and an uncommitted minor
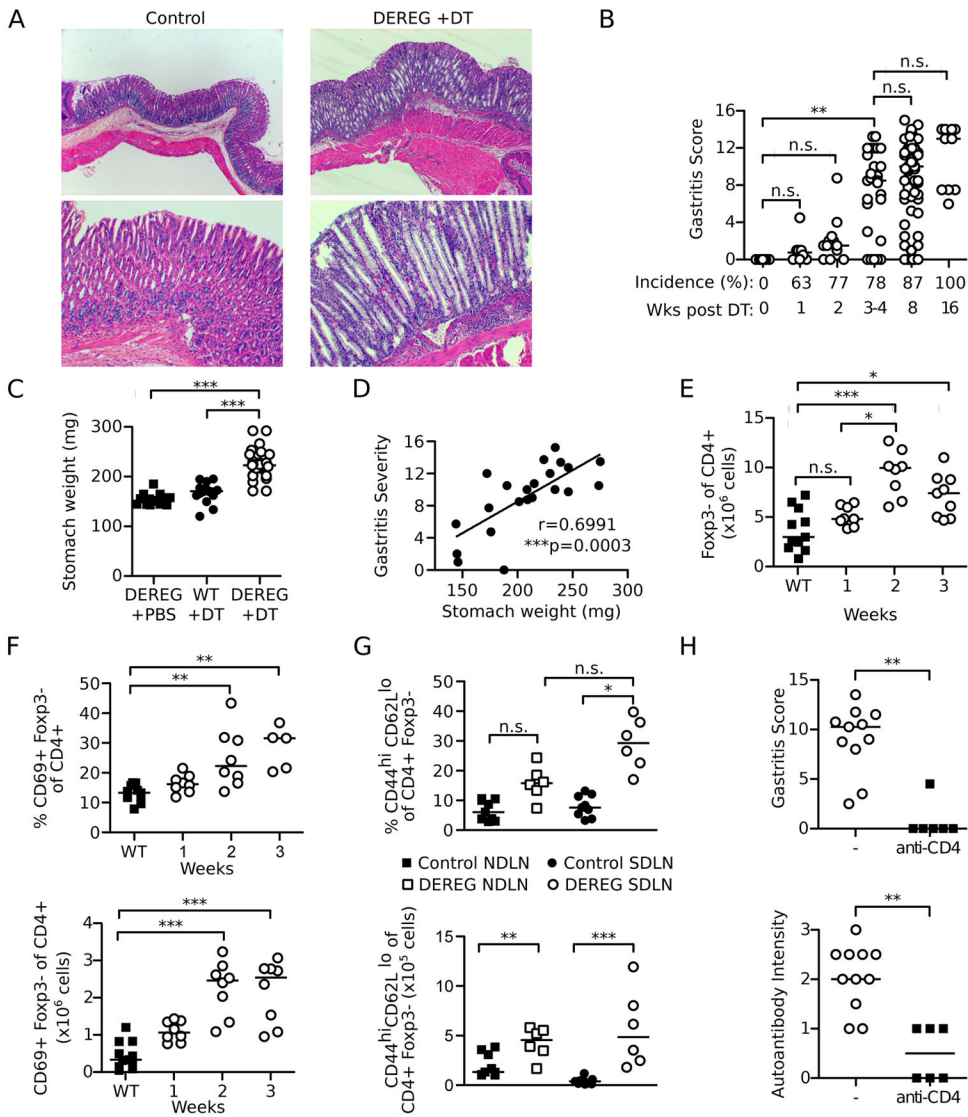
population retaining plasticity. Proc Natl Acad Sci U S A. 2009; 106:1903–8. [PubMed: 19174509]

68. Komatsu N, Okamoto K, Sawa S, Nakashima T, Oh-hora M, Kodama T, Tanaka S, Bluestone JA, Takayanagi H. Pathogenic conversion of Foxp3+ T cells into TH17 cells in autoimmune arthritis. Nat Med. 2014; 20:62–8. [PubMed: 24362934]

69. Zheng Y, Chaudhry A, Kas A, deRoos P, Kim JM, Chu TT, Corcoran L, Treuting P, Klein U, Rudensky AY. Regulatory T-cell suppressor program co-opts transcription factor IRF4 to control T(H)2 responses. Nature. 2009; 458:351–6. [PubMed: 19182775]

70. Levine AG, Arvey A, Jin W, Rudensky AY. Continuous requirement for the TCR in regulatory T cell function. Nat Immunol. 2014; 15:1070–8. [PubMed: 25263123]

71. Finkelman FD I, Katona M, Mosmann TR, Coffman RL. IFN-gamma regulates the isotypes of Ig secreted during in vivo humoral immune responses. J Immunol. 1988; 140:1022–7. [PubMed: 3125247]

72. Finkelman FD I, Katona M, Urban JF, Holmes J, Ohara J, Tung AS, Sample JV, Paul WE. IL-4 is required to generate and sustain in vivo IgE responses. J Immunol. 1988; 141:2335–41. [PubMed: 2459206]

73. Finkelman FD, Holmes J, Katona IM, Urban JF, Beckmann MP, Park LS, Schooley KA, Coffman RL, Mosmann TR, Paul WE. Lymphokine control of in vivo immunoglobulin isotype selection. Annu Rev Immunol. 1990; 8:303–33. [PubMed: 1693082]

74. Swain SL, Weinberg AD, English M, Huston G. IL-4 directs the development of Th2-like helper effectors. J Immunol. 1990; 145:3796–806. [PubMed: 2147202]

75. Grünig G, Warnock M, Wakil AE, Venkayya R, Brombacher F, Rennick DM, Sheppard D, Mohrs M, Donaldson DD, Locksley RM, Corry DB. Requirement for IL-13 independently of IL-4 in experimental asthma. Science. 1998; 282:2261–3. [PubMed: 9856950]

76. Curran DR, Cohn L. Advances in mucous cell metaplasia: a plug for mucus as a therapeutic focus in chronic airway disease. Am J Respir Cell Mol Biol. 2010; 42:268–75. [PubMed: 19520914]

77. Cohn L, Homer RJ, MacLeod H, Mohrs M, Brombacher F, Bottomly K. Th2-induced airway mucus production is dependent on IL-4Ralpha, but not on eosinophils. J Immunol. 1999; 162:6178–83. [PubMed: 10229862]

78. Possa SS, Leick EA, Prado CM, Martins MA, Tibério IFLC. Eosinophilic inflammation in allergic asthma. Front Pharmacol. 2013; 4:46. [PubMed: 23616768]

79. Davoine F, Lacy P. Eosinophil cytokines, chemokines, and growth factors: emerging roles in immunity. Front Immunol. 2014; 5:570. [PubMed: 25426119]

80. Lee JJ, Dimina D, Macias MP, Ochkur SI, McGarry MP, O'Neill KR, Protheroe C, Pero R, Nguyen T, Cormier SA, Lenkiewicz E, Colbert D, Rinaldi L, Ackerman SJ, Irvin CG, Lee NA. Defining a link with asthma in mice congenitally deficient in eosinophils. Science. 2004; 305:1773–6. [PubMed: 15375267]

81. Riiser A. The human microbiome, asthma, and allergy. Allergy Asthma Clin Immunol. 2015; 11:35. [PubMed: 26664362]

82. Wu W, Liu H-P, Chen F, Liu H, Cao AT, Yao S, Sun M, Evans-Marin HL, Zhao Y, Zhao Q, Duck LW, Elson CO, Liu Z, Cong Y. Commensal A4 bacteria inhibit intestinal Th2-cell responses through induction of dendritic cell TGF-β production. Eur J Immunol. 2016

83. Josefowicz SZ, Niec RE, Kim HY, Treuting P, Chinen T, Zheng Y, Umetsu DT, Rudensky AY. Extrathymically generated regulatory T cells control mucosal TH2 inflammation. Nature. 2012; 482:395–9. [PubMed: 22318520]

84. Gao Y, Nish SA, Jiang R, Hou L, Licona-Limón P, Weinstein JS, Zhao H, Medzhitov R. Control of T helper 2 responses by transcription factor IRF4-dependent dendritic cells. Immunity. 2013; 39:722–32. [PubMed: 24076050]

85. Williams JW, Tjota MY, Clay BS, Vander Lugt B, Bandukwala HS, Hrusch CL, Decker DC, Blaine KM, Fixsen BR, Singh H, Sciammas R, Sperling AI. Transcription factor IRF4 drives dendritic cells to promote Th2 differentiation. Nat Commun. 2013; 4:2990. [PubMed: 24356538]

86. Ulges A, Klein M, Reuter S, Gerlitzki B, Hoffmann M, Grebe N, Staudt V, Stergiou N, Bohn T, Brühl TJ, Muth S, Yurugi H, Rajalingam K, Bellinghausen I, Tuettenberg A, Hahn S, Reißig S, Haben I, Zipp F, Waisman A, Probst HC, Beilhack A, Buchou T, Filhol-Cochet O, Boldyreff B,

Breloer M, Jonuleit H, Schild H, Schmitt E, Bopp T. Protein kinase CK2 enables regulatory T cells to suppress excessive TH2 responses in vivo. Nat Immunol. 2015; 16:267–75. [PubMed: 25599562]

87. Agersborg SS, Garza KM, Tung KS. Intestinal parasitism terminates self tolerance and enhances neonatal induction of autoimmune disease and memory. Eur J Immunol. 2001; 31:851–9. [PubMed: 11241290]

88. Pochanke V, Hatak S, Hengartner H, Zinkernagel RM, McCoy KD. Induction of IgE and allergic-type responses in fur mite-infested mice. Eur J Immunol. 2006; 36:2434–45. [PubMed: 16909433]

89. Scarff KJ, Pettitt JM, Van Driel IR, Gleeson PA, Toh BH. Immunization with gastric H+/K(+)-ATPase induces a reversible autoimmune gastritis. Immunology. 1997; 92:91–8. [PubMed: 9370929]

90. Barrett SP, Gleeson PA, de Silva H, Toh BH, van Driel IR. Interferon-gamma is required during the initiation of an organ-specific autoimmune disease. Eur J Immunol. 1996; 26:1652–5. [PubMed: 8766575]

91. Stummvoll GH, DiPaolo RJ, Huter EN, Davidson TS, Glass D, Ward JM, Shevach EM. Th1, Th2, and Th17 effector T cell-induced autoimmune gastritis differs in pathological pattern and in susceptibility to suppression by regulatory T cells. J Immunol. 2008; 181:1908–16. [PubMed: 18641328]

92. Tu E, Ang DKY, Bellingham SA, Hogan TV, Teng MWL, Smyth MJ, Hill AF, van Driel IR. Both IFN-γ and IL-17 are required for the development of severe autoimmune gastritis. Eur J Immunol. 2012; 42:2574–83. [PubMed: 22777705]

93. Racke MK. Cytokine-induced immune deviation as a therapy for inflammatory autoimmune disease. J Exp Med. 1994; 180:1961–1966. [PubMed: 7525845]

94. Elias D, Meilin A, Ablamunits V, Birk OS, Carmi P, Konen-Waisman S, Cohen IR. Hsp60 Peptide Therapy of NOD Mouse Diabetes Induces a Th2 Cytokine Burst and Downregulates Autoimmunity to Various -Cell Antigens. Diabetes. 1997; 46:758–765. [PubMed: 9133541]

95. Tisch R, Wang B, Serreze DV. Induction of glutamic acid decarboxylase 65-specific Th2 cells and suppression of autoimmune diabetes at late stages of disease is epitope dependent. J Immunol. 1999; 163:1178–87. [PubMed: 10415012]

96. Raphael I, Nalawade S, Eagar TN, Forsthuber TG. T cell subsets and their signature cytokines in autoimmune and inflammatory diseases. Cytokine. 2014; 74:5–17. [PubMed: 25458968]

97. McHugh RS, Shevach EM, Margulies DH, Natarajan K. A T cell receptor transgenic model of severe, spontaneous organ-specific autoimmunity. Eur J Immunol. 2001; 31:2094–103. [PubMed: 11449363]

98. Candon S, McHugh RS, Foucras G, Natarajan K, Shevach EM, Margulies DH. Spontaneous organ-specific Th2-mediated autoimmunity in TCR transgenic mice. J Immunol. 2004; 172:2917–24. [PubMed: 14978094]

99. Lafaille JJ, Keere FV, Hsu AL, Baron JL, Haas W, Raine CS, Tonegawa S. Myelin basic protein-specific T helper 2 (Th2) cells cause experimental autoimmune encephalomyelitis in immunodeficient hosts rather than protect them from the disease. J Exp Med. 1997; 186:307–12. [PubMed: 9221760]

100. Pakala SV, Kurrer MO, Katz JD. T Helper 2 (Th2) T Cells Induce Acute Pancreatitis and Diabetes in Immune-compromised Nonobese Diabetic (NOD) Mice. J Exp Med. 1997; 186:299–306. [PubMed: 9221759]

101. Lou YH, Park KK, Agersborg S, Alard P, Tung KS. Retargeting T cell-mediated inflammation: a new perspective on autoantibody action. J Immunol. 2000; 164:5251–7. [PubMed: 10799886]

102. Poulin M, Haskins K. Induction of diabetes in nonobese diabetic mice by Th2 T cell clones from a TCR transgenic mouse. J Immunol. 2000; 164:3072–8. [PubMed: 10706696]

103. Bettington M, Brown I. Autoimmune gastritis: novel clues to histological diagnosis. Pathology. 2013; 45:145–9. [PubMed: 23277173]

104. Bedeir AS, Lash RH, Lash JG, Ray MB. Significant increase in IgG4+ plasma cells in gastric biopsy specimens from patients with pernicious anaemia. J Clin Pathol. 2010; 63:999–1001. [PubMed: 20924031]

105. Lundgren M, Persson U, Larsson P, Magnusson C, Smith CI, Hammarström L, Severinson E. Interleukin 4 induces synthesis of IgE and IgG4 in human B cells. Eur J Immunol. 1989; 19:1311–5. [PubMed: 2788092]

106. Gascan H, Gauchat JF, Roncarolo MG, Yssel H, Spits H, de Vries JE. Human B cell clones can be induced to proliferate and to switch to IgE and IgG4 synthesis by interleukin 4 and a signal provided by activated CD4+ T cell clones. J Exp Med. 1991; 173:747–50. [PubMed: 1997653]

107. Punnonen J, Aversa G, Cocks BG, McKenzie AN, Menon S, Zurawski G, de Waal Malefyt R, de Vries JE. Interleukin 13 induces interleukin 4-independent IgG4 and IgE synthesis and CD23 expression by human B cells. Proc Natl Acad Sci U S A. 1993; 90:3730–4. [PubMed: 8097323]

108. Lahner E, Annibale B. Pernicious anemia: new insights from a gastroenterological point of view. World J Gastroenterol. 2009; 15:5121–8. [PubMed: 19891010]

109. Fulkerson PC, Rothenberg ME. Targeting eosinophils in allergy, inflammation and beyond. Nat Rev Drug Discov. 2013; 12:117–29. [PubMed: 23334207]

110. Jacobsen EA, Ochkur SI, Pero RS, Taranova AG, Protheroe CA, Colbert DC, Lee NA, Lee JJ. Allergic pulmonary inflammation in mice is dependent on eosinophil-induced recruitment of effector T cells. J Exp Med. 2008; 205:699–710. [PubMed: 18316417]

111. Chu DK, Jimenez-Saiz R, Verschoor CP, Walker TD, Goncharova S, Llop-Guevara A, Shen P, Gordon ME, Barra NG, Bassett JD, Kong J, Fattouh R, McCoy KD, Bowdish DM, Erjefält JS, Pabst O, Humbles AA, Kolbeck R, Waserman S, Jordana M. Indigenous enteric eosinophils control DCs to initiate a primary Th2 immune response in vivo. J Exp Med. 2014; 211:1657–72. [PubMed: 25071163]

112. Jacobsen EA, Zellner KR, Colbert D, Lee NA, Lee JJ. Eosinophils regulate dendritic cells and Th2 pulmonary immune responses following allergen provocation. J Immunol. 2011; 187:6059–68. [PubMed: 22048766]

113. Jin H, Park Y, Elly C, Liu YC. Itch expression by Treg cells controls Th2 inflammatory responses. J Clin Invest. 2013; 123:4923–34. [PubMed: 24135136]

114. Sekiya T, Kondo T, Shichita T, Morita R, Ichinose H, Yoshimura A. Suppression of Th2 and Tfh immune reactions by Nr4a receptors in mature T reg cells. J Exp Med. 2015; 212:1623–40. [PubMed: 26304965]

115. Blair PJ, Bultman SJ, Haas JC, Rouse BT, Wilkinson JE, Godfrey VL. CD4+CD8− T cells are the effector cells in disease pathogenesis in the scurfy (sf) mouse. J Immunol. 1994; 153:3764–74. [PubMed: 7930593]

116. Kanangat S, Blair P, Reddy R, Daheshia M, Godfrey V, Rouse BT, Wilkinson E, Deheshia M. Disease in the scurfy (sf) mouse is associated with overexpression of cytokine genes. Eur J Immunol. 1996; 26:161–5. [PubMed: 8566060]

117. Clark LB, Appleby MW, Brunkow ME, Wilkinson JE, Ziegler SF, Ramsdell F. Cellular and molecular characterization of the scurfy mouse mutant. J Immunol. 1999; 162:2546–54. [PubMed: 10072494]

118. Chatila TA, Blaeser F, Ho N, Lederman HM, Voulgaropoulos C, Helms C, Bowcock AM. JM2, encoding a fork head-related protein, is mutated in X-linked autoimmunity-allergic disregulation syndrome. J Clin Invest. 2000; 106:R75–81. [PubMed: 11120765]

119. Lahl K, Mayer CT, Bopp T, Huehn J, Loddenkemper C, Eberl G, Wirnsberger G, Dornmair K, Geffers R, Schmitt E, Buer J, Sparwasser T. Nonfunctional regulatory T cells and defective control of Th2 cytokine production in natural scurfy mutant mice. J Immunol. 2009; 183:5662–72. [PubMed: 19812199]

120. Buzzelli JN, Chalinor HV, Pavlic DI, Sutton P, Menheniott TR, Giraud AS, Judd LM. IL33 Is a Stomach Alarmin That Initiates a Skewed Th2 Response to Injury and Infection. C Cell Mol Gastroenterol Hepatol. 2015; 1:203–221.e3.

121. Sojka DK, Huang YH, Fowell DJ. Mechanisms of regulatory T-cell suppression - a diverse arsenal for a moving target. Immunology. 2008; 124:13–22. [PubMed: 18346152]

122. Walker LSK. Regulatory T cells overturned: the effectors fight back. Immunology. 2009; 126:466–74. [PubMed: 19278420]

123. D'Alise AM, Auyeung V, Feuerer M, Nishio J, Fontenot J, Benoist C, Mathis D. The defect in T-cell regulation in NOD mice is an effect on the T-cell effectors. Proc Natl Acad Sci U S A. 2008; 105:19857–62. [PubMed: 19073938]

124. Gregori S, Giarratana N, Smiroldo S, Adorini L. Dynamics of pathogenic and suppressor T cells in autoimmune diabetes development. J Immunol. 2003; 171:4040–7. [PubMed: 14530324]

125. You S, Belghith M, Cobbold S, Alyanakian MA, Gouarin C, Barriot S, Garcia C, Waldmann H, Bach JF, Chatenoud L. Autoimmune diabetes onset results from qualitative rather than quantitative age-dependent changes in pathogenic T-cells. Diabetes. 2005; 54:1415–22. [PubMed: 15855328]

126. Korn T, Reddy J, Gao W, Bettelli E, Awasthi A, Petersen TR, Bäckström BT, Sobel RA, Wucherpfennig KW, Strom TB, Oukka M, Kuchroo VK. Myelin-specific regulatory T cells accumulate in the CNS but fail to control autoimmune inflammation. Nat Med. 2007; 13:423–31. [PubMed: 17384649]

127. Monk CR, Spachidou M, Rovis F, Leung E, Botto M, Lechler RI, Garden OA. MRL/Mp CD4+, CD25− T cells show reduced sensitivity to suppression by CD4+, CD25+ regulatory T cells in vitro: a novel defect of T cell regulation in systemic lupus erythematosus. Arthritis Rheum. 2005; 52:1180–4. [PubMed: 15818683]

128. Vargas-Rojas MI, Crispín JC, Richaud-Patin Y, Alcocer-Varela J. Quantitative and qualitative normal regulatory T cells are not capable of inducing suppression in SLE patients due to T-cell resistance. Lupus. 2008; 17:289–94. [PubMed: 18413409]

129. Venigalla RKC, Tretter T, Krienke S, Max R, Eckstein V, Blank N, Fiehn C, Ho AD, Lorenz HM. Reduced CD4+, CD25− T cell sensitivity to the suppressive function of CD4+, CD25high, CD127 -/low regulatory T cells in patients with active systemic lupus erythematosus. Arthritis Rheum. 2008; 58:2120–30. [PubMed: 18576316]

130. Schneider A, Rieck M, Sanda S, Pihoker C, Greenbaum C, Buckner JH. The effector T cells of diabetic subjects are resistant to regulation via CD4+ FOXP3+ regulatory T cells. J Immunol. 2008; 181:7350–5. [PubMed: 18981158]

131. Wehrens EJ, Mijnheer G, Duurland CL, Klein M, Meerding J, van Loosdregt J, de Jager W, Sawitzki B, Coffer PJ, Vastert B, Prakken BJ, van Wijk F. Functional human regulatory T cells fail to control autoimmune inflammation due to PKB/c-akt hyperactivation in effector cells. Blood. 2011; 118:3538–48. [PubMed: 21828127]

132. Pace L, Rizzo S, Palombi C, Brombacher F, Doria G. Cutting edge: IL-4-induced protection of CD4+CD25− Th cells from CD4+CD25+ regulatory T cell-mediated suppression. J Immunol. 2006; 176:3900–4. [PubMed: 16547222]

133. Pillemer BBL, Qi Z, Melgert B, Oriss TB, Ray P, Ray A. STAT6 activation confers upon T helper cells resistance to suppression by regulatory T cells. J Immunol. 2009; 183:155–63. [PubMed: 19535633]

134. Yang S, Fujikado N, Kolodin D, Benoist C, Mathis D. Immune tolerance. Regulatory T cells generated early in life play a distinct role in maintaining self-tolerance. Science. 2015; 348:589–94. [PubMed: 25791085]

135. Campbell DJ. Control of Regulatory T Cell Migration, Function, and Homeostasis. J Immunol. 2015; 195:2507–13. [PubMed: 26342103]

Figure 1. Transient Treg cell depletion results in AIG dependent on CD4+ T cells
(A) Representative stomach histology showing well-organized mucosa (control mice, left) or hypertrophy, abundant mucin-positive cells, and reduction in parietal cells (Treg cell-depleted DEREG mice, right) (H&E stain; top, x40; bottom, x100). (B) Kinetics of gastritis incidences and severity after Treg cell depletion. (C) Stomach weights at 3 weeks. (D) Correlation of gastritis score and stomach weight at 3 weeks. (E) Kinetics of absolute numbers of Foxp3− of CD4+ T cells and (F) percentages (top) and absolute numbers (bottom) of CD69+ Foxp3− of CD4+ T cells in pooled lymph nodes after Treg cell depletion. (G) Percentages (top) and absolute numbers (bottom) of CD44hiCD62Llo of CD4+Foxp3− cells in the NDLN and SDLN at 3 weeks in control and Treg cell-depleted DEREG mice. (H) Gastritis score and gastric autoantibody intensity of mice at 8 weeks after Treg cell depletion with or without anti-CD4 depleting antibody treatment. Data were pooled from 2–11 independent experiments per time point. Each symbol represents an individual

mouse. *p<0.05, **p<0.01, ***p<0.001; Kruskal-Wallis tests with Dunns posttests (B, C, E, F, G top); Mann-Whitney t test (G bottom, H); Spearman Correlation test (D).
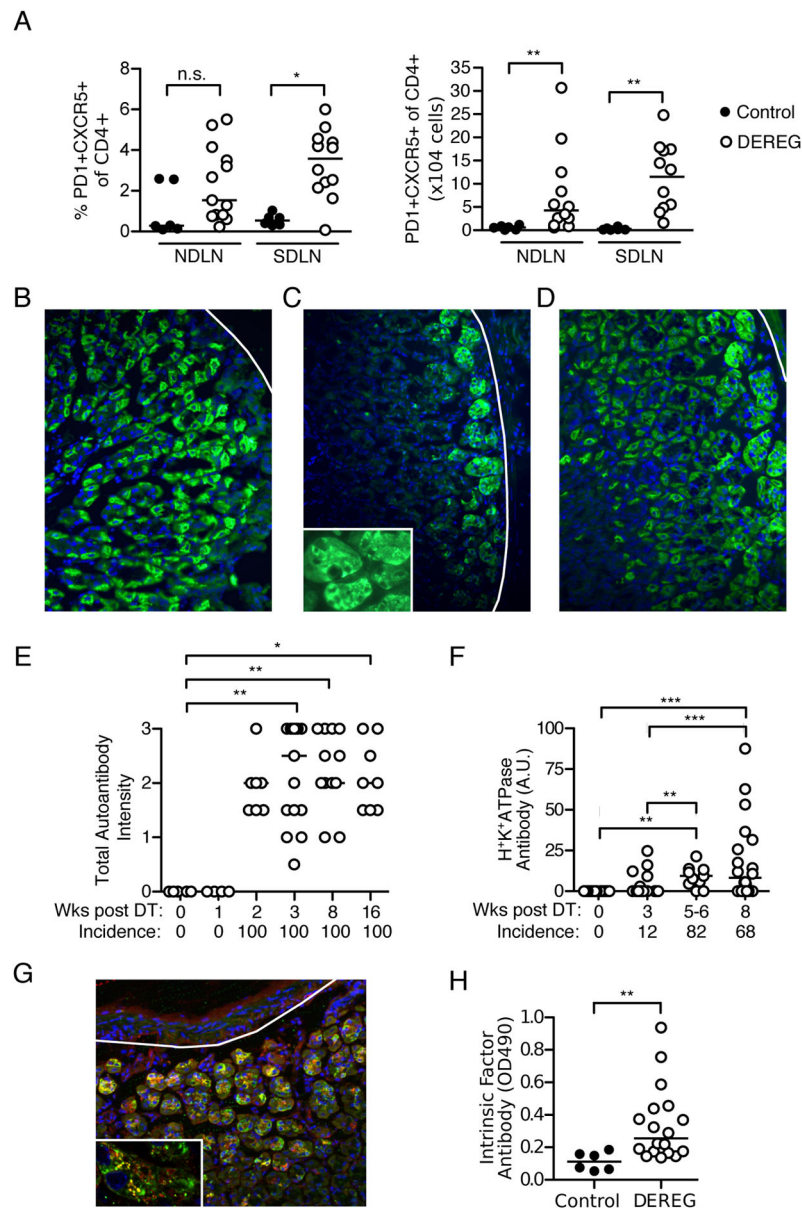
Figure 2. Tfh cell and autoantibody responses in Treg cell-depleted DEREG mice with AIG
(A) Percentages (left) and absolute numbers (right) of PD1+CXCR5+CD4+ T cells in the NDLN and SDLN at 3 weeks in control and Treg cell-depleted DEREG mice. (B–D) Immunofluorescence patterns of serum gastric autoantibodies from Treg cell-depleted mice: (B) parietal cells only, (C) basal gland epithelial cells only, or (D) both cell types (green, IgG; blue, DAPI; x200; white lines denote base of gastric mucosa). Inset in C shows patchy cytoplasmic distribution. (E) Kinetics of total serum gastric IgG autoantibody incidences and staining intensities after Treg cell depletion detected by immunofluorescence. (F) Kinetics of gastric $H^+K^+ATPase$ autoantibody incidence and titer after Treg cell depletion (ELISA). (G) Co-localization (yellow) of DEREG mouse serum autoantibody to basal gland epithelial cells (green) with anti-human IF antibody (red), detected by immunofluorescence on normal stomach sections (blue, DAPI; x200; white line denote base of gastric mucosa). Punctate

pattern of co-localization is shown as yellow dots in inset (x800). (H) ELISA detection of IF autoantibody in control and Treg cell-depleted mice at 3 weeks. The latter mice were selected based on the presence of autoantibodies directed to basal gland epithelial cells (present in 69% of mice). Data were pooled from 2–11 independent experiments per time point. Each symbol represents an individual mouse. *p<0.05, **p<0.01, ***p<0.001; Kruskal-Wallis tests with Dunns posttests (E, F); Mann-Whitney t test (A, H).
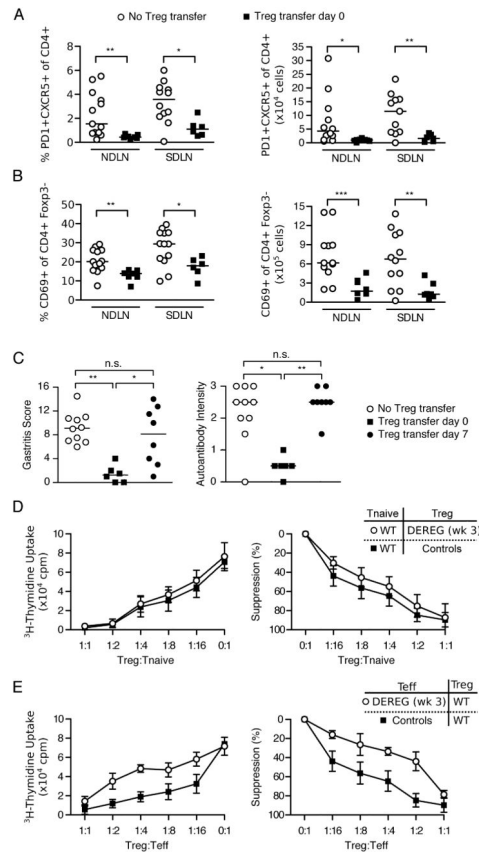
Figure 3. Effector T cells from DEREG mice with transient Treg cell depletion are less sensitive to suppression by Treg cells *in vitro* and *in vivo*

Percentages (left) and absolute numbers (right) of (A) PD1+CXCR5+ of CD4+ T follicular helper cells or (B) CD69+ of CD4+Foxp3− activated T cells in the NDLN or SDLN at 3 weeks in Treg cell-depleted DEREG mice with (filled squares) or without (empty circles) WT Treg cell reconstitution at day 0 of DT treatment. (C) Gastritis score (left) and gastric IgG autoantibody intensity (right) at 3 weeks in Treg cell-depleted DEREG mice with or without infusion of WT Treg cells at day 0 or day 7 after the first dose of DT treatment. (D) Suppression of naïve CD4+CD25− T cell proliferation by CD4+CD25+ Treg cells from WT mice or from the SDLN of DEREG mice obtained at 3 weeks after DT treatment. (E) Suppression of proliferation of CD4+CD25− T cells from WT mice or from the SDLN of DEREG mice obtained at 3 weeks after DT treatment by CD4+CD25+ Treg cells from WT mice. Proliferation of CD4+CD25− T cells in D and E was assessed by uptake of [^{3}H]thymidine (representative mean and standard deviations of cpm from 5 wells each in 1 experiment, left; average percent suppression of 2–3 experiments, right). p = 0.0950 in D, p = 0.0280 in E (three-way ANOVA with F-test). Data in A–C were pooled from 3 independent experiments and each symbol represents an individual mouse. *p<0.05, **p<0.01, ***p<0.001; Kruskal-Wallis test with Dunns posttests (C) or Mann-Whitney t tests (A, B).
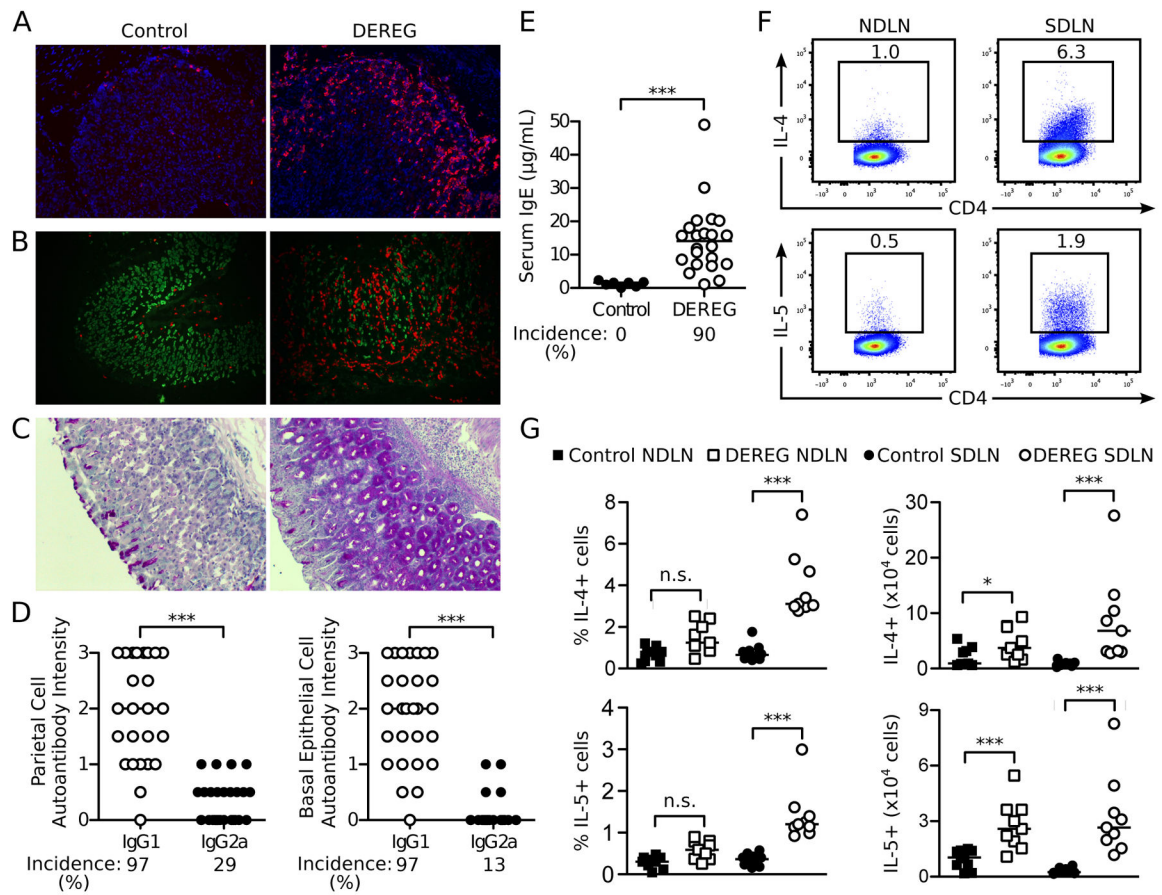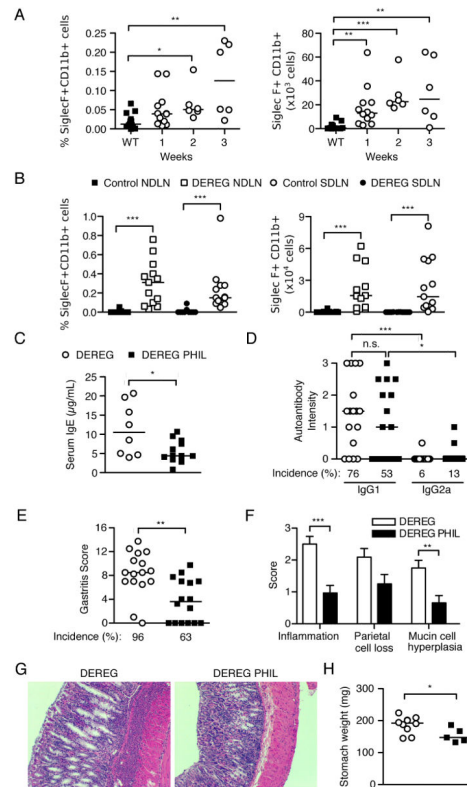
Figure 4. AIG in Treg cell-depleted DEREG mice is predominantly associated with Th2 cell responses

(A) Representative immunofluorescence microscopy images of eosinophils in the stomach mucosa from control (left) and Treg cell-depleted mice (right) at 1 week (red, SiglecF; blue, DAPI; x200). (B) Co-localization of parietal cells and eosinophils in representative immunofluorescence microscopy images of stomach mucosa from control (left) and Treg cell-depleted DEREG mice with AIG (right) (red, SiglecF; green, mouse serum antibody to gastric parietal cells; x200). (C) Mucin-positive cells in stomach sections from control (left) and Treg cell-depleted mice (right) at 3 weeks (Periodic acid-Schiff stain; x100). (D) Intensity and prevalence of serum IgG1 and IgG2a autoantibodies to parietal cells (left) and basal epithelial cells (right) from DEREG mice detected by indirect immunofluorescence. (E) Total serum IgE levels and prevalence in control and Treg cell-depleted DEREG mice. (F) Representative flow cytometry dot plots of IL-4 and IL-5 producing CD4+ T cells in the SDLN and NDLN of Treg cell-depleted DEREG mice at 3 weeks (cells were stimulated *ex vivo* by PMA and ionomycin before flow cytometry analysis). (G) Quantitation of F (left: percentage; right: absolute number). Data were pooled from 3 (F, G), 4 (E), and 6 (D) independent experiments. Each symbol represents an individual mouse. *p<0.05, **p<0.01, ***p<0.001; Kruskal-Wallis tests with Dunns posttest (G left); Mann-Whitney t tests (D, E, G right).
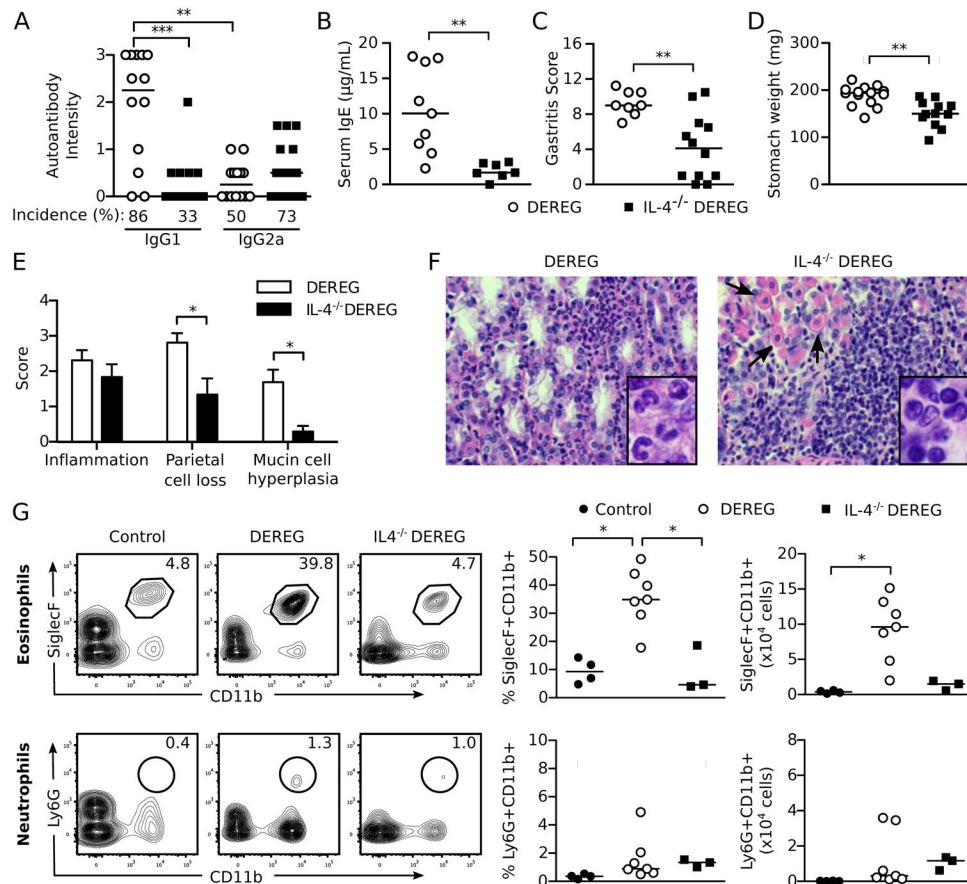
Figure 5. IL-4 contributes to AIG pathogenesis in Treg cell-depleted DEREG mice
(A) Serum IgG1 and IgG2a gastric autoantibody staining intensities by immunofluorescence, (B) serum IgE levels, (C) total gastritis score, (D) stomach weights, (E) score of individual histopathologic findings of AIG in the stomach, and (F) stomach infiltrating cells (H&E x400; arrows indicate residual parietal cells) of IL-4-sufficient DEREG and IL-4$^{-/-}$ DEREG mice at 3 weeks. Insets (enlarged from x1000): note the numerous granulocytes in stomachs of IL-4$^{-/-}$ DEREG mice (left) and the numerous mononuclear cells in the IL-4-sufficient DEREG mice (right). (G) Flow cytometric analysis of SiglecF+CD11b+ eosinophils (top) and Ly6G+CD11b+ neutrophils (bottom) isolated from stomachs of control mice and Treg cell-depleted WT and IL-4$^{-/-}$ DEREG mice at 3 weeks. Representative plots (left) were gated on live CD45+ cells (numbers indicate percentages of cells in the gates). Percent (center) and absolute numbers (right) of eosinophils and neutrophils are quantified. Data were pooled from 3 (G), 4 (B–E), and 7 (A) independent experiments. Each symbol represents an individual mouse (A–E) or a pool from 3 mice (G). *p<0.05, **p<0.01, ***p<0.001; Kruskal-Wallis tests with Dunns posttests (A, G); Mann-Whitney t tests (B–E).

Figure 6. Eosinophils contribute to AIG pathogenesis in Treg cell-depleted DEREG mice
(A) Kinetics of SiglecF+CD11b+ eosinophil expansion in pooled lymph nodes as percentage (left) and absolute number (right). (B) Percentage (left) and absolute number (right) of eosinophils in the NDLN and SDLN of control and Treg cell-depleted DEREG mice at 3 weeks. (C) Serum IgE levels, (D) serum IgG1 and IgG2a gastric autoantibody staining intensities, (E) Gastritis severity and prevalence, (F) score of individual histopathologic findings of AIG in stomach, (G) representative stomach histopathology (H&E, x100), and (H) stomach weights in DEREG mice (open symbols) and eosinophil-deficient DEREG PHIL mice (filled symbols) at 3 weeks. Data were pooled from 5 (A) or 7 (B–H) independent experiments. Each symbol represents an individual mouse. *p<0.05, **p<0.01, ***p<0.001; Mann-Whitney t tests (B right, C, E, F, H); Kruskal-Wallis tests with Dunns posttest (A, B left, D).
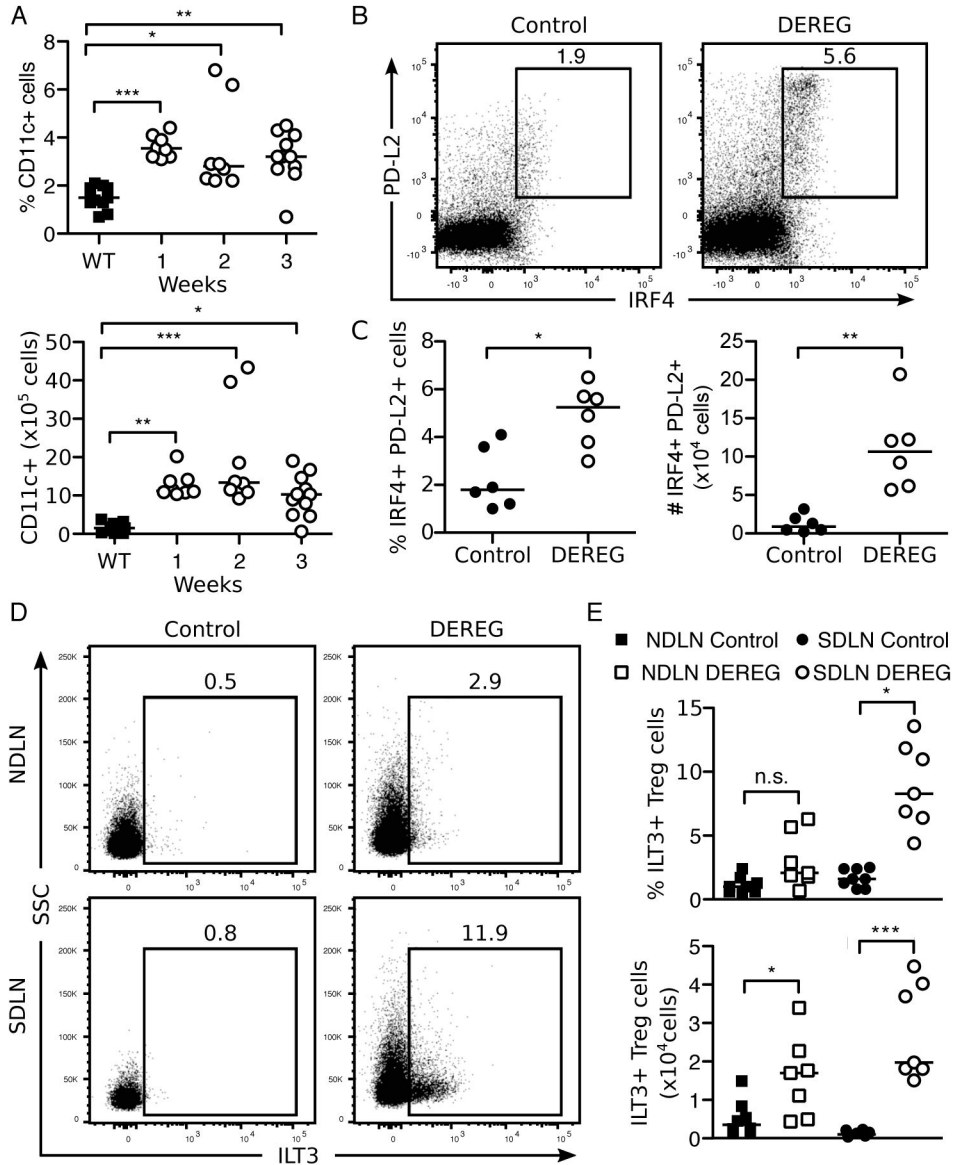
Figure 7. Increase in Th2-promoting PD-L2+IRF4+ dendritic cell subsets as well as ILT3+ Treg cell subsets in transiently Treg-cell depleted DEREG mice

(A) Kinetics of the percentage (top) and absolute number (bottom) of live, CD11c+ dendritic cells in pooled lymph nodes. (B) Representative flow cytometry dot plots (top, numbers indicate percentages of cells in the gates) and quantitation as percentage (bottom, left) and absolute number (bottom, right) of IRF4+PD-L2+ dendritic cells among live, CD4−, CD11c+, MHCII+ cells in pooled SDLN and NDLN of control and Treg cell-depleted DEREG mice at 1 week. (C) Representative flow cytometry dot plots (left, numbers indicate percentages of cells in the gates) and quantitation as percentage (top, right) and absolute number (bottom, right) of ILT3+ Treg cells among live, CD4+, Foxp3+ cells in the SDLN or NDLN of control and Treg cell-depleted DEREG mice at 3 weeks. Data were pooled from 2 (B), 3 (C), or 5 (A) independent experiments. Each symbol represents an individual mouse.

*p<0.05, **p<0.01, ***p<0.001; Mann-Whitney t tests (B, C bottom); Kruskal-Wallis tests with Dunns posttest (A, B top).